Femtosecond Cr^{2+}-Based Lasers

Irina T. Sorokina and Evgeni Sorokin

(Invited Paper)

***Abstract*—We review a novel class of femtosecond Cr^{2+}-doped ZnSe and ZnS lasers, which operates in a very important for applications wavelength range between 2 and 3.5 μm and which generates ultrashort optical pulses that are only five optical cycles in duration. Room-temperature Cr^{2+}-lasers provide tens of Watts average power, >70% slope efficiency, ultrabroad tunability (~1400 nm between 2 and 3.4 μm) in the continuous wave regime and GW-level peak powers in the amplified femtosecond regime. Different mode-locking techniques from Kerr-lens to graphene saturable absorbers have been demonstrated, and dispersion compensation methods from bulk materials to chirped mirrors allowed the realization of self-starting few-optical cycle oscillators and the demonstration of a number of applications in spectroscopy and nonlinear optics. The Watt level few-optical cycle Cr:ZnS oscillator[1] operating at 2.4 μm is distinguished by extremely short pulse duration of only 41 fs, hundreds of kilowatt peak powers, and tens of nanojoule pulse energies. Using the direct diode-pumping or fiber laser pump sources such a laser can be made reliable and compact, which paves the way to industrial realisation and applications in environmental analysis, oil and gas sensing, hazardous gas detection, breath analysis, fine material processing of semiconductors, composite materials, and glasses.**

***Index Terms*—Laser, mid-infrared, near-infrared, optical pulse generation, laser mode-locking, laser tuning, sensors, chemical hazards, gas detectors.**

I. Introduction

ROOM-temperature solid-state lasers based on Cr^{2+}-doped II-VI compound materials like ZnSe or ZnS are in many respects similar to the Ti:sapphire laser, but offer the ability to generate high-power broadly tunable radiation in the mid-infrared (mid-IR) wavelength range above 2 μm. This wavelength range, which is often called a "molecular fingerprint" region, and in particular, the range between 2 and 5 μm, is characterized by the presence of strong fundamental and overtone vibrational absorption lines of major atmospheric constituents, as well as several important for industrial and medical applications molecules and radicals (see Figs. 1 and 2). The ability of Cr^{2+}- lasers to spectrally cover in a single shot or by rapid laser tuning the widest possible wavelength range that contain many molecular absorption lines, is the main advantage of this class of compact mid-IR lasers.

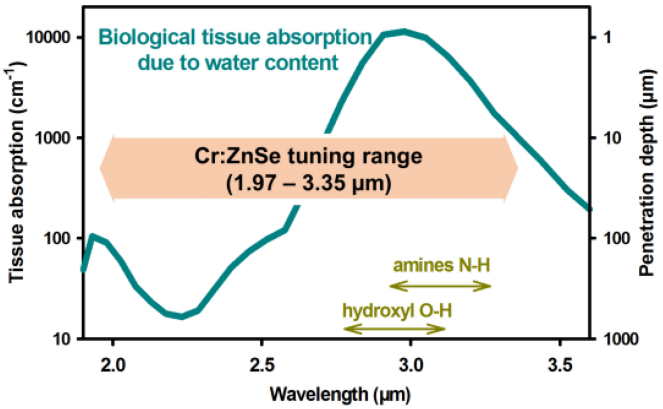

Fig. 1. Typical absorption and penetration depth of the biological tissue, as well as the absorption ranges of some important radicals [1].

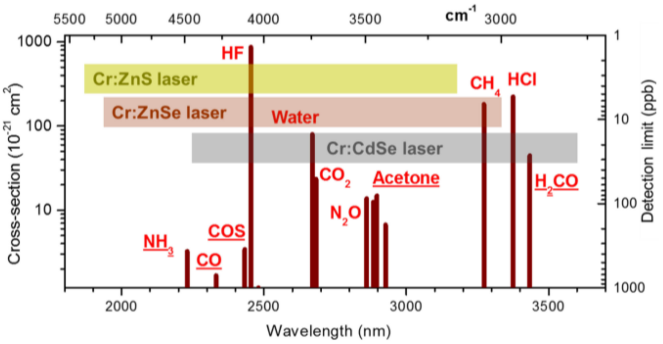

Fig. 2. Spectral coverage and tunability of the most representative Cr^{2+}-lasers and spectral positions of the measured trace gas absorption lines with the corresponding minimum detectable gas concentrations—results of photoacoustic measurements [2]–[4]. For many of important molecules the detection limit lies well in the ppb (part-per-billion) region.

As can be seen in Fig. 2, the absorption lines include, e.g.: water vapor (H_2O), which fills the whole range between 2.5 and 3 μm and has a maximum around 2.7 μm, carbon monoxide (CO) with strong features around 2.3–2.4 μm, carbon dioxide (CO_2) absorbing around 2.7–2.8 μm, nitrous oxide (N_2O), methane (CH_4), carbohydrates, and other oil and petroleum associated gases having several absorption features all through 2–4 μm range, as well as many other species. Detection of low concentrations of these molecules for the purpose of medical, environmental or industrial diagnostics, e.g. diagnostics of the human breath, or of oil and petroleum associated gases is currently done using laser systems, which are based mainly on

Manuscript received April 19, 2014; revised June 9, 2014; accepted June 30, 2014. This work was supported in part by the Austrian Science Fund Project P24916, the EU-FET GRAPHENICS under Grant 618086, and the Norwegian Research Council Projects FRITEK/191614 and the Nano 2021 Project N219686.

I. T. Sorokina is with the Department of Physics, Norwegian University of Science and Technology, Trondheim, 7491 Norway (e-mail: sorokina@ntnu.no).

E. Sorokin is with the Photonics Institute, Vienna University of Technology, 1040 Wien, Austria (e-mail: sorokin@tuwien.ac.at).

Color versions of one or more of the figures in this paper are available online at http://ieeexplore.ieee.org.

Digital Object Identifier 10.1109/JSTQE.2014.2341589

[1]Patent pending, ATLA Lasers AS, Trondheim, Norway.

single gas detection semiconductor or quantum cascade laser devices or on nonlinear optical conversion techniques. The latter include optical parametric oscillators (OPO) and difference frequency generators. OPO has much appeal as an ideal broadband solution for remote sensing and multigas analysis, but is by construction rather complex and costly. In the same wavelength range, Cr^{2+}-lasers are a single-stage devices, which provide very broad spectral coverage both as narrow-linewidth tunable and as broadband sources. For example, a femtosecond Cr:ZnS supercontinuum source generates spectra, which cover the whole wavelength range between 2 and 3 μm [5], [6]. In competition to traditional femtosecond OPO technology, femtosecond Cr^{2+}-lasers offer the versatility and robustness of compact fiber laser pumped solid-state lasers, and as such are ready for real-world applications such as trace gas sensing and breath analysis (see Section VI), medicine as well as fine material processing.

Various spectroscopic techniques—femtosecond Fourier transform (FT) spectroscopy [7]–[10] and dual-comb FT spectroscopy [11]–[13]—have been realized and successfully verified using these femtosecond sources, with sensitivities achieving ppb and potentially parts-per-trillion levels, which are otherwise not achievable with the present multi-species gas sensor technologies (see Section VI). In addition, these lasers might be perfect ultrahigh peak power mid-IR sources for X-Ray generation [1], [14], [15].

This review encompasses mainly the works on femtosecond Cr^{2+}:ZnSe laser technology development between 1997 and 2014 in our group in Vienna, as well as highlights a few of our most recent works on Cr^{2+}:ZnS laser development in Trondheim. In the last few years a tremendous leap forward in femtosecond pulse generation in both, Cr^{2+}:ZnSe as well as Cr^{2+}:ZnS has been made by several leading groups in the field. There is a considerable research effort on Cr^{2+}:ZnSe femtosecond technology led the A. Sennaroglu group at Koç University, P. Moulton group at Q-Peak Inc., and by S. Mirov group at the University of Alabama Birmingham. The coherent efforts in this direction led to real world applications demonstrations of this novel class of femtosecond lasers, proving the viability of this technology and opening new avenues towards their applications, some of which are described in Section VI.

The paper is organized as follows: starting with the motivation and historical introduction (see Section II), it provides the background in continuous-wave (CW) tunable operation (see Section III), further describing the principles and most recent advances in generation and applications of ultrashort pulses and frequency combs directly from the solid-state oscillator based on Cr^{2+}:ZnSe (see Section IV) as well as Cr:ZnS laser (see Section V) and highlights radical efficiency, breadth of wavelength coverage and sensitivity increase when applied to high-resolution molecular spectroscopy and trace gas sensing (see Section VI).

II. Motivation and Historical Perspective

Cr^{2+} - femtosecond laser technology is a result of more than 18 years of research and development effort, which starts from the discovery of the new class of Cr^{2+} - doped II-VI compound laser materials and realization of the first pulsed lasers by the group of pioneers from the Lawrence Livermore Laboratory back in 1995 [16]–[20], through first CW tunable operation in Cr^{2+}:ZnSe in 1999 [21], [22] and then in Cr^{2+}:ZnS [23], [24] to the first actively and passively mode-locked picosecond [25] and then femtosecond Cr^{2+}:ZnSe laser operation in 2006 [26].

The main motivation for the research and development of Cr^{2+}-based femtosecond laser technology has been a surprising similarity of spectroscopic, material and laser properties of these lasers with those of the Ti:sapphire laser—a "work horse" of femtosecond technology. Due to these extraordinary properties of Cr:ZnSe and Cr:ZnS, their inventors and at that time leaders of the Livermore laser group, W. F. Krupke and S. A. Payne referred to these materials as "Ti:sapphire of the mid-infrared" and as being "without precedent" [27].

Indeed, the electric-dipole transitions of the Cr^{2+}-ions, occupying tetrahedral sites without inversion symmetry, are characterized by large oscillator strength and short lifetime. The high activation energy in Cr:ZnSe and Cr:ZnS crystals leads to the decreased nonradiative decay rate and to the high fluorescence quantum yield [28]. Moreover, the excited state absorption (ESA) to the higher energy levels is spin-forbidden in these materials leading to the negligibly low ESA [29], which is a common plague of the vibronic materials [30].

It is therefore not a surprise that these materials drew such an attention of both, research and industry, as first room-temperature broadly tunable CW lasers operating between 2 and 3 μm [21], [23], [31], [32] and later on as sources of high power ($>$20 W average power) and high energy ($>$20 mJ at 7 ns and $>$1 J at 7 ms) pulsed operation [33], [34], GW peak power amplified femtosecond operation [35] and since recently, also Watt level few optical cycle femtosecond operation [36], [37] and ultrabroad tunability between 1.95 and 3.35 μm [38].

III. CW Performance of Cr:ZnSe and Cr:ZnS

The remarkable properties of the Cr^{2+}:ZnSe and Cr^{2+}:ZnS crystals, described in the previous Section, such as high emission cross-section, negligibly low ESA, good chemical and mechanical stability, and thermal conductivity being nearly as high as in sapphire gave these material enormous potential as an active medium for CW tunable mid-infrared lasers. For a detailed review of the experiments performed so far, we refer the reader to the following review articles [37], [39]–[42]. Here we focus on the material and CW laser properties of single crystal and polycrystalline Cr:ZnSe and Cr:ZnS with the final aim to obtain high-efficiency and high-power femtosecond pulse operation to be described in Sections IV and V.

A. Materials

One of the most important advantages of Cr:ZnSe and Cr:ZnS is the commercial availability of the technologically developed and low-cost polycrystalline material. The existing technologies for producing ceramic crystals, such as chemical vapor deposition method or the hot-press method of powders result in high optical quality substrates—typical window material for CO_2 lasers. This makes Cr:ZnSe and Cr:ZnS one of the most

technological and low-cost active media among the known solid-state lasers. In our works we have been using both, single crystal as well as ceramic (polycrystalline) materials. The undoped crystals of Cr:ZnSe and Cr:ZnS have been grown by various methods like e.g. the Bridgman, physical vapor transport (PVT), and chemical vapor transport methods. The best laser results have been obtained from crystals grown by the Bridgman and PVT methods. The high structural quality of the single crystals grown under optimum growth conditions has been confirmed by X-ray diffraction.

Chromium was introduced by thermal diffusion from solid metal source. The advantages of this doping method [43]–[46] over the growth of the crystal containing Cr from the beginning is the ability to precisely control dopant level by the adjustment of the diffusion temperature and duration of the treatment. Diffusion was typically carried out in the argon atmosphere in evacuated (5×10^{-6} Torr) fused silica ampoules in the temperature range 800–1000 °C during 3–10 days depending on the crystal. We used a commercially available metallic chromium of 99.99% purity. The Cr^{2+} concentration was estimated to vary between 5×10^{18} ions/cm^3 to 2×10^{19} ions/cm^3 by comparing the absorption coefficient of our sample to the absorption cross-section reported in [19], [20]. The disadvantage of diffusion doping over the growth of the Cr-doped crystals are the Cr^{2+} ion concentration gradient along the diffusion depth and surface erosion. Nevertheless, this method allows one to obtain good quality 2–3 mm thick samples with fair Cr homogeneity, which is sufficient for CW as well as femtosecond lasers.

The good chemical and mechanical stability of the host material and its thermal conductivity nearly, which is nearly as high as in sapphire, ranks Cr^{2+}:ZnSe and Cr^{2+}:ZnS crystals very high among other broadband solid-state lasers. The only significant issue of these materials is the relatively high thermal lensing parameter dn/dT ($\sim 70 \cdot 10^{-6}$ K^{-1} in Cr:ZnSe, $46 \cdot 10^{-6}$ K^{-1} in ZnS compared to $12 \cdot 10^{-6}$ K^{-1} in sapphire [47]). However, the latter is partially compensated by the three times longer wavelength and hence three times larger beam area, as well as by the possibility to reduce the relative Stokes shift by long-wavelength pumping [29], [48], [49].

Among all II–VI chalcogenides ZnS is distinguished by the largest energy gap of 3.8 eV, the smallest lattice constant and by the correspondingly blue-shifted emission cross-section, which peaks around 2.35 μm (Fig. 4). While working with this crystal we established that the formally cubic crystal of Cr^{2+}:ZnS exhibited birefringence [23], [24]. The X-ray analysis revealed the partial hexagonal symmetry in the crystal. However, the structure of the crystals was not that of wurtzite, but a modification of the cubic zinc blende. Cr^{2+}:ZnS is one of the most structurally rich polytypical compounds and can exist in several structure types, sphalerite and wurtzite structures being the most common. Thus, even the so called cubic Cr:ZnS as a rule reveals a certain degree of "hexagonality", which amounts up to 10–20%. The cause of the hexagonal symmetry may be due to twinning and fault-stacking enhanced by the Cr-doping in case of the melt grown Cr^{2+}:ZnS. This natural degree of "hexagonality" has certain implications on the tuning, which will be discussed later.

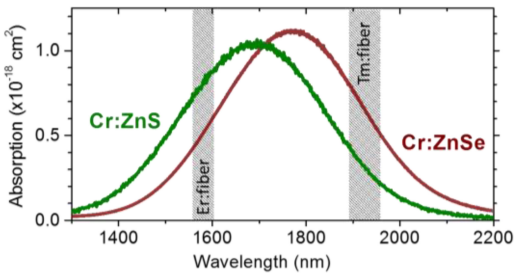

Fig. 3. Absorption cross-section spectra of Cr:ZnSe and Cr:ZnS with operating ranges of commercial fiber laser pump sources.

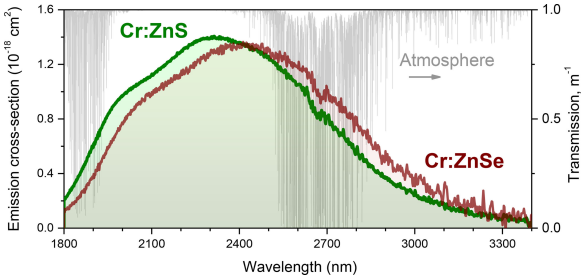

Fig. 4. Emission cross-section spectra of Cr:ZnSe and Cr:ZnS. The grey spectrum shows atmospheric transmission for 1 m path at normal conditions.

Cr^{2+}:ZnS is also distinguished by the lowest dn/dT, the highest hardness and damage threshold among other Cr^{2+}-doped media, which makes it attractive for high power applications. The power handling capability of Cr:ZnS is comparable to that of Yb:YAG—the factor of three larger Stokes shift is compensated by the three times higher thermal conductivity. From the power scaling point of view Cr:ZnS is thus as interesting as Yb:YAG and in a thin-disk design with reduced thermal lens sensitivity can approach the same power levels as other thin-disk lasers.

B. Spectroscopy

ZnSe and related compounds attracted a lot of attention back in the 60s and 70s as materials for blue LEDs and diodes. Spectroscopy of Cr^{2+} ($3d^4$) in chalcogenides has been subject of extensive research since the early 1960's [50]–[52]. Curiously, the main interest in chromium as an impurity in ZnSe producing deep levels has been due to the quenching of photoluminescence (recombination luminescence). Therefore Cr was frequently referred to as a visible luminescence "killer". However, these fundamental studies and availability of good optical quality undoped material have laid a solid foundation for the spectroscopic investigations of Cr^{2+} as an active laser ion. For detailed spectroscopic studies the reader is referred to previous reviews [19], [30], [39], [40], [47], [53], [54].

Here we would like to pay attention to the spectroscopic features, which are most important for broadband operation and ultrashort-pulsed generation. The absorption and emission spectra in Cr:ZnSe and Cr:ZnS are depicted in Figs. 3 and 4, respectively. The broad absorption band is centered around

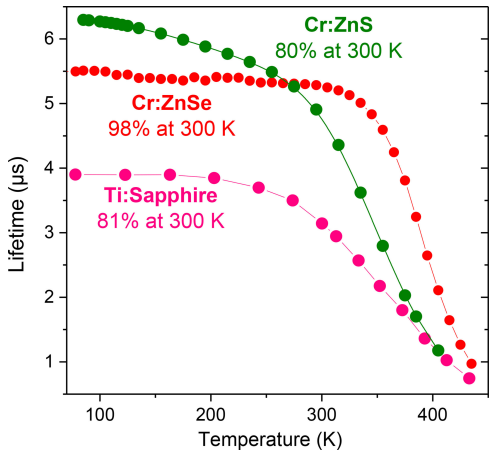

Fig. 5. Temperature dependent life-time measurements for Cr:ZnS, Cr:ZnSe and Ti:sapphire.

1.78 μm in Cr:ZnSe, and around 1.67 μm in Cr:ZnS, which make them particularly attractive for pumping with Tm-fiber and Er-fiber lasers respectively (see Fig. 3). The broad-band emission between 2 and 3 μm (see Fig. 4) reflects the parity-forbidden yet spin-allowed electronic transition between ^{5}E and ^{5}T$_2$ states. As can be seen in Fig. 4, Cr:ZnS better matches the transparency window, while Cr:ZnSe can be used to operate further into the infrared.

It is important to underline the role of the Jahn-Teller effect. The Jahn–Teller splittings of the ground ^{5}T$_2$ state and of the excited ^{5}E state are 340 and 40 cm^{-1}, respectively [55]. Contrary to Ti:sapphire, the ground state is split more than the upper state, which favors triple peaks in the fluorescence spectrum of Cr^{2+} ions and a correspondingly broader gain spectrum. This makes Cr^{2+}-based materials the broadest among all existing lasers.

The activation-energy and multiphonon relaxation processes set the fundamental limit for obtaining CW room-temperature laser operation from vibronic transitions in the mid-IR region [28]. Therefore, the life-time measurements gain a special importance (see Fig. 5). Here, Cr:ZnSe demonstrates a constant lifetime well beyond room temperature, while Cr:ZnS lifetime shortens by 20% at 300 K, like in Ti:Sapphire. Note that the lifetime data in [19] provide much higher values at room temperature due to the obvious reabsorption influence. The curves in Fig. 5 have been recorded with special care to avoid reabsorption effects.

The four-level scheme and favorable lifetime temperature dependence suggest a rather low pump threshold at room temperature. In addition, the infrared wavelength generally favors a lower threshold according to the fundamental scaling rule $I_{\rm th} \propto (\Delta\lambda/\lambda)\,\lambda^{-4}$ [28], so that pumping thresholds of a few tens of mW are quite common, despite the large value of the $\Delta\lambda/\lambda \sim 0.37$, which exceeds that of the Ti:sapphire [28]. From the point of view of ultrashort pulse generation, relative bandwidth defines the minimum number of optical cycles per pulse. This implies that achieving two optical cycle pulse durations, corresponding to 16 fs at 2.5 μm (analogous to 5 fs in Ti:sapphire), is feasible.

C. Diode-Pumping

The low pump threshold of Cr:ZnSe and Cr:ZnS makes direct diode pumping feasible. Direct diode-pumping has been demonstrated in pulsed [56] and CW [57]–[62] regimes with the use of a variety of 1.6–1.9 μm InGaAsP/InP and GaSb based diode-lasers. The direct diode-pumping normally yields smaller cost and better wall plug efficiency lasers, but represents a challenge for mode-locked operation. Nevertheless, a femtosecond diode-pumped Cr:ZnSe laser has been demonstrated in [63].

For power scaling of the diode-pumped operation, thin disk arrangement is of interest, as it allows pumping with low beam quality sources. There have been two successful experimental attempts to realize a thin-disk Cr:ZnSe laser [64]–[67], with the best results currently reaching 5 and 4 Watts of output power under Tm:fiber and direct diode pumping, respectively, and some limited tuning [66]. High thermal lensing and softness of Cr:ZnSe limit further power scaling. Thermal quenching of emission at temperatures above room temperature is another limiting factor that could lead to thermal runaway [68]. Thermal quenching is not a problem for low and medium power operation in both Cr:ZnSe or Cr:ZnS. However, at high power operation the better thermo-optical properties of Cr:ZnS prevail (in equal setups, the latter emits over 20 W as compared to 5 W output by Cr:ZnSe [34]), and this advantage should also remain in the diode-pumped thin-disk design. For the sake of completeness we should mention here the possibility of pumping using a VECSEL (thin-disk semiconductor laser) [48], [49].

D. Ultrabroad CW Tunable Operation

The promising spectroscopic characteristics of Cr^{2+}- based materials stimulated intensive laser related research. Soon after the first experimental demonstration of the Cr^{2+}:ZnSe laser its performance was greatly improved, spanning tuning ranges of several hundreds of nanometers [21], [32], [39] at close to the quantum limit slope efficiency (>60%), with narrow linewidth and power levels in excess of 2 W in CW regime [1] and 20 Watts (up to 30 W) in the pulsed regime [33], [34].

The possibility of wide tuning has always been an aim of almost every report on CW and pulsed operation of Cr^{2+}-based lasers [21], [23], [24], [32], whereas the limitation has been due to the optics rather than to the active medium. In particular, Cr^{2+}:ZnSe has been shown to operate from 2.0 to 3.1 μm in the CW regime with two different sets of optics [39] and from 1880 to 3100 in the pulsed regime with four sets of optics [69].

Ultrabroadband operation is extremely attractive for various applications. Besides the direct use of the tunable narrow-linewidth operation for spectroscopic and sensor applications, demonstration of the broad tuning range is extremely important for the few-cycle femtosecond operation and frequency comb generation, as a proof of the active medium gain properties and availability of optics. In [38] we presented the ultrabroadband tunable laser operation of ceramic and single-crystalline Cr:ZnSe and Cr:ZnS materials, using the novel hybrid mirrors covering a record tuning range of over 1400 nm range with a single set of optics, and generating over 600 mW of output power. The mirrors have been designed and prepared using a

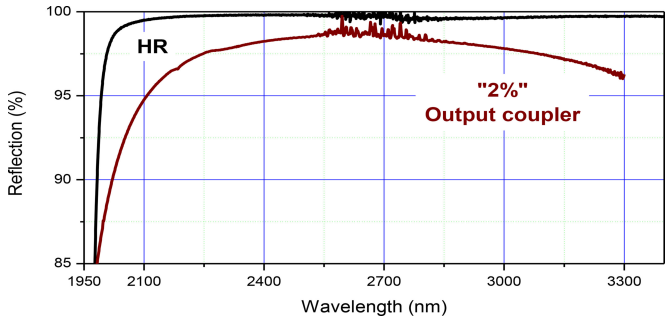

Fig. 6. Hybrid design mirror reflectivity curves. HR – high reflectivity mirror.

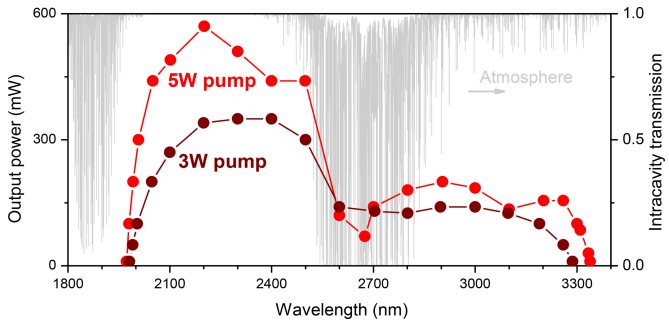

Fig. 7. Tuning of the ceramic Cr:ZnSe laser with a CaF2 prism. The maximum tuning range is 1973 – 3339 nm at 10 mW level.

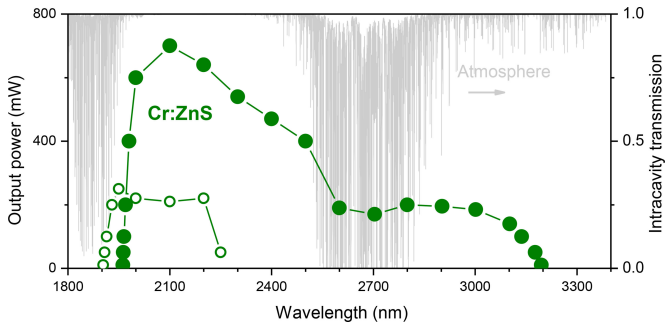

Fig. 8. Tuning of the ceramic Cr:ZnS laser with a ZnSe prism. The tuning range is 1962–3195 nm at 10 mW level. Open circles: Additional set of optics to reach 1904 nm at the short-wavelength side.

hybrid technology, which combines semiconductor and dielectric materials. This allowed the increase of the index contrast and hence the bandwidth of the mirrors (see Fig. 6). The experimental results are shown in Figs. 7 – 9, together with the intracavity atmospheric transmission, explaining the tuning curve "dip" between 2.5 and 2.9 μm.

Interestingly, the tuning curve of a cubic single crystalline Cr:ZnS laser was found to be modulated by a Lyot-filter action of the gain medium. The residual birefringence is due to the stacking faults in ZnS, as discussed in Section III-A. In the single crystal, even the very weak but regularly orientated birefringence accumulates on the 2–3 mm path, which creates a significant effect. In a polycrystalline material with a random grain orientation, the birefringence produces only a weak

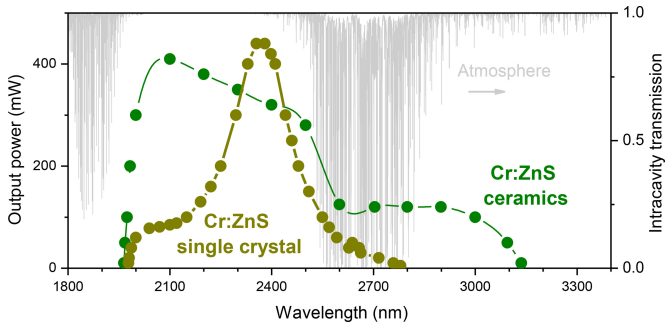

Fig. 9. Tuning of a ceramic and single-crystal Cr:ZnS lasers.

wavelength-independent depolarization loss. As a result, the ceramic material may give a broader and more uniform tuning than a single crystal (see Fig. 9). The demonstrated extreme bandwidth of the gain and of the optics opens up the way to single-cycle operation in the mode-locked femtosecond regime.

IV. Ultrashort-Pulsed Cr:ZnSe and Cr:ZnS Lasers

The extremely broad gain and high third-order nonlinearity in Cr:ZnSe and Cr:ZnS (n_2 is 60–30 times higher than in Ti^{3+}:sapphire [70]–[72]) makes this material suitable for generation of the few- to single-cycle pulses. Such pulses in the mid-infrared spectral region can be used as unique diagnostic tools for investigation of numerous transient processes on the femtosecond scale as well as for such applications as remote sensing, environmental monitoring, mid-IR free space communications, optical frequency standards, optical coherence tomography [73], ophthalmology and dermatology in medicine [74]. They can be also be used for pumping mid-IR OPOs to produce even longer wavelengths [75], [76].

A. Active and Passive Mode-Locking of Cr:ZnSe Laser

Only one or two years after demonstration of the first CW lasing in Cr:ZnSe two groups demonstrated transform-limited Gaussian-shaped pulses as short as 4 ps using an acousto-optic modulator [25], [77]. The output power of 400 mW [78] was limited only by the pump source. Two years later we have developed and mode-locked in the same way the Cr:ZnSe ceramic laser [79]. Varying the modulation depth of the AOM, we produced pulses with duration between 20 and 40 ps and an average output power up to 150 mW.

In the work [25] we have also observed and studied two distinctly different regimes of operation: a purely actively mode-locked regime allowing relatively long pulses with pulse durations of the order of tens of picoseconds, as well as an alternative passive mode-locking regime taking place in the narrow range of the cavity and acousto-optic modulator parameters, allowing to obtain only ~4 ps pulses, which could not be described within the frames of Kuizenga–Siegman theory of active mode-locking [80]. Earlier a similar phenomenon has been observed in the acousto-optically initiated passively mode-locked Ti:sapphire laser, generating 2 ps pulses [81], [82]. This was the first

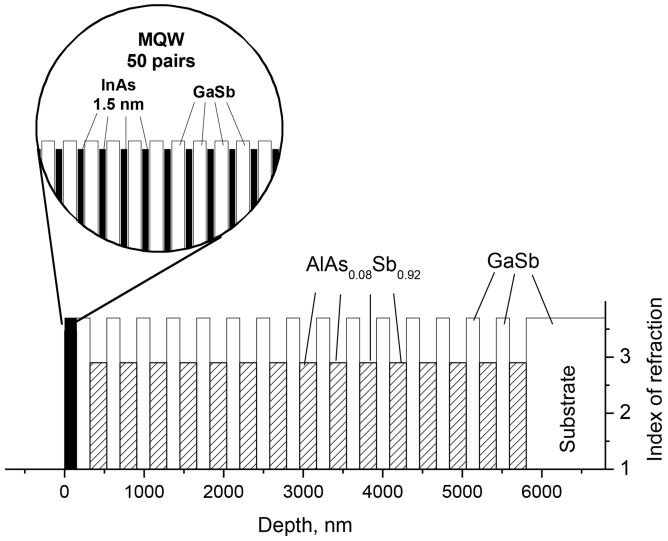

Fig. 10. Schematic of the SESAM [86].

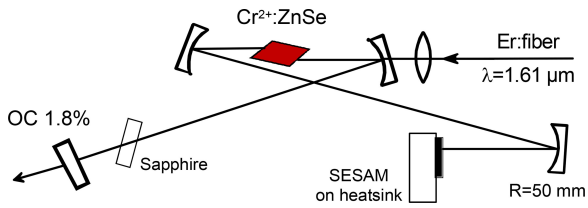

Fig. 11. Generic schematic of a SESAM-controlled Cr:ZnSe laser. The pump at 1.61 μm and the laser radiation are polarized in the plane of the figure. OC: Output coupler.

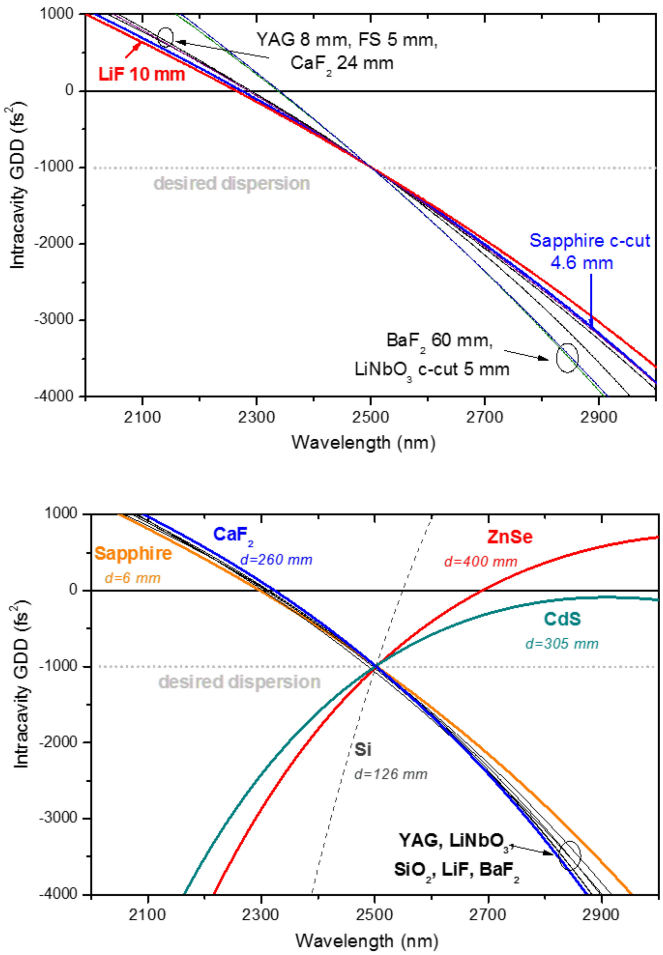

Fig. 12. Round-trip dispersion compensation using bulk (upper graph) and prism (lower graph) methods [26], [87]. All calculations assume 4 mm ZnSe active medium and -1000 fs^2 dispersion target. The control parameter is the thickness of a bulk material and the prism apex distance d.

experimental observation of the passive mode-locking in the positive dispersion regime in Cr:ZnSe laser (see Section V-C).

B. SESAM Mode-Locking of Cr:ZnSe and Cr:ZnS

Passive mode-locking of solid-state oscillators using a semiconductor saturable absorber [83] is a very versatile approach, because it contains a number of controllable design parameters and provides the self-starting ability. It is also perfectly compatible with the mid-IR lasers [84], given the possibility of band-gap engineering. In 2005 Pollock *et al*. realized the first semiconductor saturable absorber (SESAM) mode-locked Cr:ZnSe laser, generating 11 ps pulses at 2.5 μm at 400 mW output power [85]. Shortly after that we were able to passively mode-lock Cr:ZnS laser using an InAs/GaSb based multiple quantum well SESAM, generating ~1.1 ps pulses at 125 mW of output power around 2.45 μm [86]. The SESAM sample consisted of a saturable absorber based on 50 layers of InAs/GaSb quantum wells, grown on top of a dielectric mirror made from 15 alternating layers of quarter-wave thickness GaSb and $AlAs_{0.08}Sb_{0.92}$ on a GaSb substrate (see Fig. 10). The SESAM had a small-signal absorption of 12% per bounce, a calculated relaxation time of 200–300 ps, and a saturation fluence of 40 μJ/cm^2. Under similar conditions in a Cr^{2+}:ZnSe laser we obtained ~1 ps pulses at 140 mW ouput power. Adding proper dispersion compensation the first femtosecond operation was realized in Cr:ZnSe laser, generating ~100 fs pulses at up to 75 mW power around 2.5 μm wavelength [26].

The schematic of the laser was unusually simple as the dispersion compensation for the first time was achieved by using only a 3 mm thick sapphire plate (see Fig. 11). Selection of sapphire is not random: a study of possible materials for the bulk dispersion compensation shows sapphire to be second best material after LiF in terms of providing minimum round-trip third-order dispersion (see Fig. 12, upper graph). Note that using the classic Brewster-prism pair for dispersion compensation does not bring significant improvements (see Fig. 12, lower graph), with third-order dispersion values being comparable or higher than for the bulk compensators. This has been later confirmed experimentally in a study [72], where different bulk and prism materials were compared in a Kerr-Lens modelocked Cr:ZnSe laser.

Further pulse shortening requires means to improve dispersion control, compensating, at least partially, the third order. This can be done using chirped mirrors [88], a meanwhile standard approach for dispersion control and simultaneous bandwidth extension in ultrafast optics. Dispersion compensation by chirped

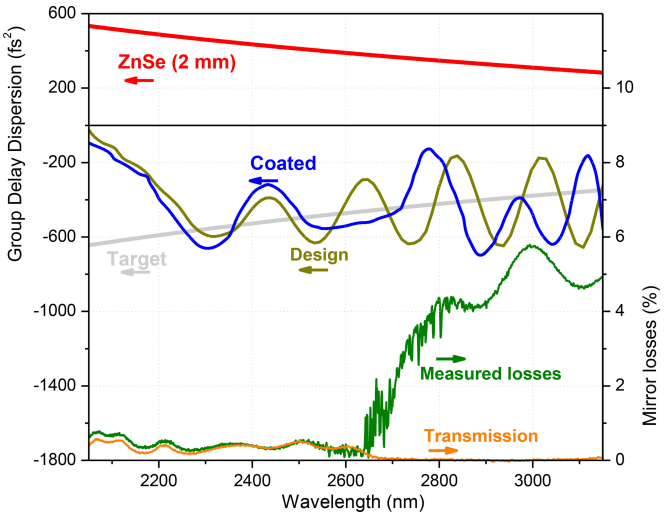

Fig. 13. Chirped mirrors for dispersion compensation of ZnSe [87]. The 53-layer mirrors were designed to provide high reflection from 2000 to 3300 nm and to compensate for 2 mm of ZnSe in single bounce. The graph shows the designed and fitted dispersion curves as well as measured absorption losses in the coating.

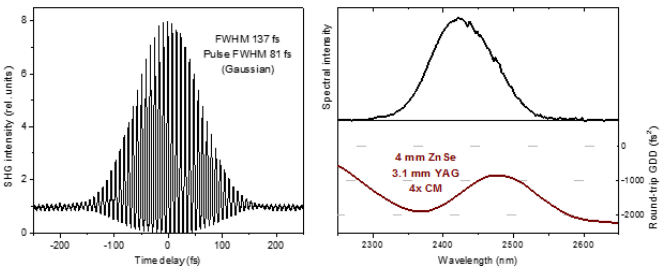

Fig. 14. Autocorrelation trace, spectrum and round-trip GDD for a hybrid-compensated Cr:ZnSe laser [87].

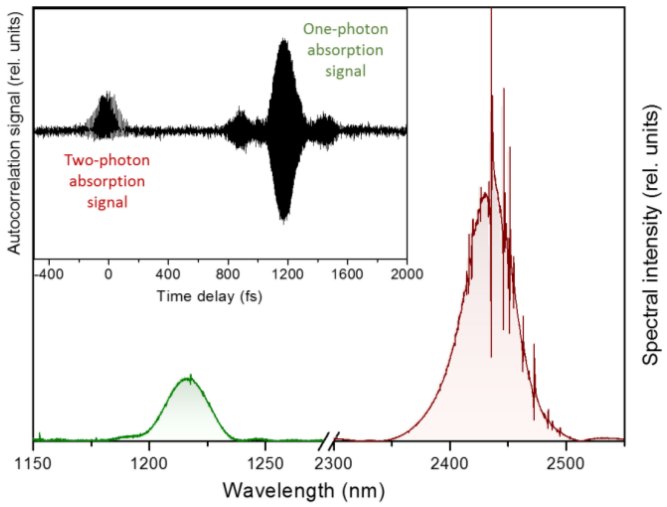

Fig. 15. Mode-locked output spectrum of the femtosecond Cr:ZnSe laser, containing the fundamental pulse (red) and the intracavity SHG signal (green). The relative intensities between the spectral parts are not to the scale. The "noise" features at the spectrum are due to the intracavity water vapor absorption lines ([92], see also Section VI-C). *Inset:* Autocorrelation trace. The second-order autocorrelation (right feature) appears smaller than the first-order autocorrelation (left feature) despite its 10^3 higher energy because the two-photon absorption in the InGaAs detector at 2.4 μm is much weaker than direct absorption at 1.2 μm.

mirrors is a challenging task in the mid-IR due to the necessity to fabricate very thick multilayer mirrors. The issues are the density control of the outer layers and impurities that accumulate during the long process. The impurities are especially detrimental at the long-wavelength side, where the optical wave must have much deeper penetration to provide negative dispersion. Fig. 13 illustrates the point: the measured in-layer absorption losses amount to 5% per bounce. The standard quarterwave stack high reflectors, manufactured in the same coating machine show less than 0.2% losses in the same spectral range. Nevertheless, this was the first successful demonstration of the broadband chirped mirrors in the mid-IR wavelength region, suitable for intracavity dispersion compensation. The best dispersion compensation turned out to be a combination of two chirped mirrors and 3.1 mm of YAG. The laser generated 80 fs pulses (ten optical cycles) at 80 mW output power at 180 MHz repetition rate (see Fig. 14). This result represents so far the shortest femtosecond pulses obtained from Cr:ZnSe oscillators.

Further extensions of the SESAM-based setup were to demonstrate femtosecond Cr:ZnSe [89] and Cr:ZnS [90] laser, based on polycrystalline (ceramic) active media. When mode-locked in the cavity of Fig. 11, both lasers routinely produced 100–110 fs (~12 optical cycles) pulses at 100–120 mW of average output power at ~200 MHz repetition rate, results being similar to those of single-crystal media (see Fig. 15). However, the complete spectrum and the autocorrelation trace in the two-photon absorption autocorrelator (see Fig. 15, inset) reveal that besides the main pulse at ~2450 nm, the laser also emits signal at second harmonic (SHG) around 1240 nm. The SHG signal can be seen in the spectrum (see Fig. 15, green trace) and in the autocorrelator, because the InGaAs detector acts as a one-photon absorber below 1700 nm. The autocorrelation trace in Fig. 15 thus contains two signals: the second-order autocorrelation with a typical 8:1 ratio (left feature) and the first-order autocorrelation, which is nearly symmetric around the baseline (right feature). The time delay between the two signals corresponds to the group delay between 2450 and 1225 nm wavelengths, accumulated in the 2-mm ZnSe beamsplitter in an unbalanced autocorrelator. With group velocity mismatch of 278 fs/mm [91], the double pass through the beamsplpitter at 45° gives 1160 fs delay, well matching the experimental observation (see Fig. 15, inset). The SH signal power is about 100–200 μW (5–10 mW intracavity) or about 10^{-3} of the main signal (0.3–0.6% intracavity conversion efficiency).

The origin of this SHG signal is the lack of central symmetry in tetrahedral zinc blende structure, giving rise to nonzero second harmonic coefficient. The intracavity SHG from the Cr:ZnSe laser in CW regime was observed before [40]. It is clear, however, that the SHG cannot be efficient in single crystal ZnSe or cubic ZnS because no birefringent phase matching is possible.

In the polycrystalline samples the situation is different. The crystal consists of multitude of differently oriented

microcrystallites, that are comparable or smaller than the ZnSe coherence length of $l_c = 22\ \mu$m, providing for the quasi-regular grating of optical inhomogeneities, making collinear SHG in ceramic Cr:ZnSe possible. From the theoretical standpoint this effect is described by a model in which a vector phase synchronism is realized in the region of normal crystal dispersion due to the contribution of the wave vector of the grating [93]. This is in every respect analogous to quasi-phase matching (QPM), except that the grains are randomly oriented and have random sizes. In this case, the random walk model applies [94]–[98]. In comparison to the QPM with a regular domain pattern, in random QPM the conversion efficiency grows *linearly* with propagation distance, but the process is *non-resonant*. Most importantly, the intensity dependence of the random QPM is still quadratic, meaning that this process may become significant limitation at shorter and more energetic pulses. In the experiment, the intracavity SHG results in certain increase of amplitude noise, but it may open up interesting application opportunities, especially in the frequency standards area.

In a recent experiment, Kerr-Lens mode-locked Cr:ZnS and Cr:ZnSe polycrystalline lasers have been demonstrated [99], however, the authors did not report about SHG issues.

V. High Power Femtosecond Laser Oscillators

Successful realization of sub-100 fs chirped mirror controlled Cr:ZnSe lasers using SESAM served as a strong motivation to explore the limits in terms of pulse duration, average power and pulse energy scaling. From the point of view of robustness and power scalability Cr:ZnS is a material of choice. As discussed in Section III, the thermo-optical properties of Cr:ZnS are better suited to power scaling, and this is confirmed in direct comparison [34]. In addition to that, twice smaller nonlinearity [40] should allow higher intracavity energies before pulse break-up.

It turns out, however, that in the SESAM mode-locked femtosecond operation substitution of Cr:ZnSe by Cr:ZnS brings only marginal improvement. In the same experimental conditions, Cr:ZnS laser produced 130 fs pulse duration at 130 mW output power (0.7 nJ pulse energy), while Cr:ZnSe laser delivered 132 fs pulse duration at 90 mW output power or 0.5 nJ pulse energy (see Fig. 16). The reason is that the SESAM is the main absorbing element (~6% unsaturable losses), thus limiting the efficiency and power handling capacity. Increasing the intracavity power resulted in deterioration of the beam quality, loss of mode-locking stability, and eventually the SESAM damage [100]. The SESAM is also the main frequency-filtering element [see Fig. 17(a)] and, most importantly, it is also the main source of the higher-order dispersion [see Fig. 17(b)]. Resolving this constraint requires either a SESAM-free operation such as Kerr-lens mode-locking (KLM), thus sacrificing the self-starting ability, or finding an appropriate saturable absorber which does not impose power and bandwidth limitations. In what follows, we shall consider both approaches.

A. Watt-Level KLM Cr:ZnS Laser

KLM [101] makes use of the spatial variation of the resonator beam profile due to self-focusing caused by the Kerr

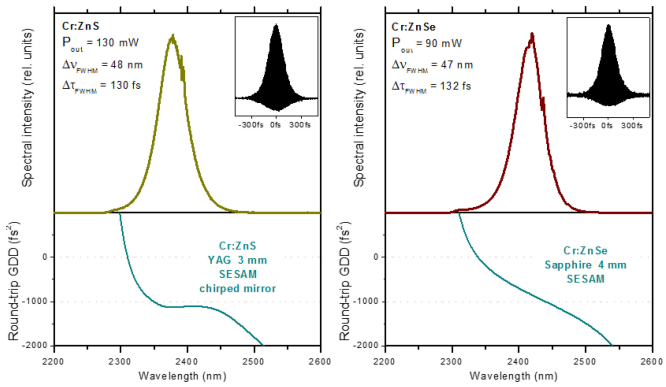

Fig. 16. Comparison of SESAM mode-locked Cr:ZnS and Cr:ZnSe lasers (adapted from [100]).

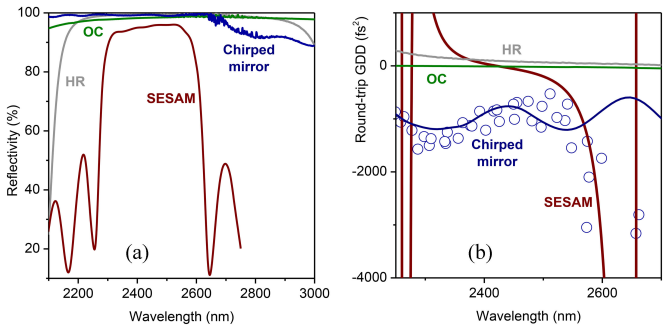

Fig. 17. (a) Mirror transmission and (b) dispersion in SESAM-controlled Cr:ZnSe and Cr:ZnS lasers (adapted from [100]).

effect inside the medium. Together with the soft aperture effect, produced by the gain profile in longitudinally-pumped setup, self-focusing results in the self-amplitude modulation (SAM) leading to mode-locking [102]. Since the original publications, the KLM lasers has become the mainstream of ultrashort-pulse technology, providing the highest output power and shortest pulses due to the fact that there is no absorbers or bandwidth-limiting elements in the cavity. At the same time, the KLM performance is now defined by the parameters of the active medium, such as gain saturation intensity and third-order nonlinearity, and in most cases the pulsed operation requires external initiation.

KLM operation in Cr:ZnSe lasers has been reported in 2009 by the two groups independently [103], [104]. In our first reported experiment [104] we used the chirped mirror dispersion control and obtained 300 mW of output power at ~200 MHz repetition rate and 100 fs pulse duration. The limitation was obviously due to the third-order dispersion, because any attempt to reduce the dispersion resulted into spontaneous switching to the chaotic positive dispersion regime, later studied in detail in [105]. To the contrary, the setup, reported in [103], used Tm-fiber pump and the prism dispersion compensation and produced 95-fs pulses with 40 mW of output power at 94 MHz repetition rate, later improved to 165 mW with 121 fs pulse duration [72]. Recently, KLM operation has been demonstrated

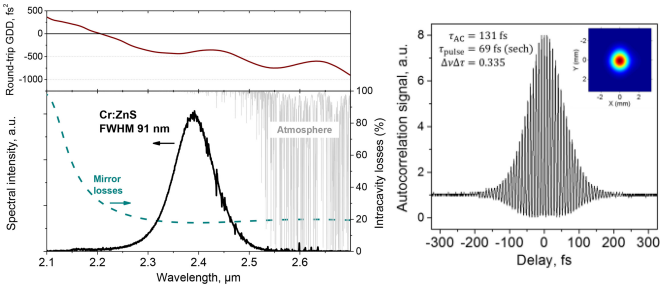

Fig. 18. (a) Output spectrum of a femtosecond Cr:ZnS laser (black), calculated round-trip GDD (dark red), and intracavity losses due to the mirrors (blue-green dashed) and atmospheric absorption (gray). (b) Autocorrelation trace and beam cross-section of the KLM Cr:ZnS laser pulses at highest output power (adapted from [106]).

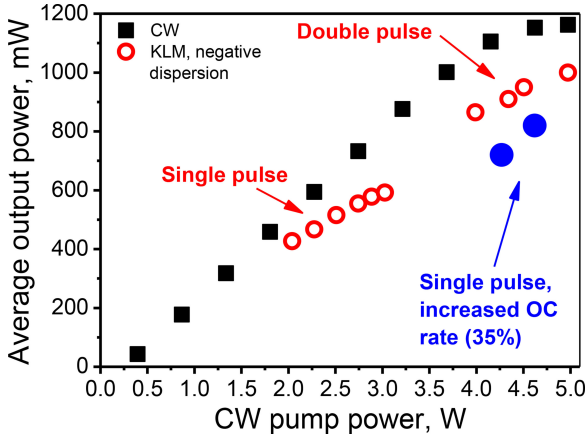

Fig. 19. Output characteristics of the KLM Cr:ZnS laser in CW (black), in single pulse and double pulse regimes (red). The maximum out power in the single pulse regime was 820 mW (blue).

also in a polycrystalline Cr:ZnSe oscillator under Er:fiber laser pumping delivering up to 30 mW of 126-fs pulses [99].

Significantly higher output power could be obtained with Cr:ZnS active medium. We used a 2.5 mm thick PVT grown and diffusion doped Cr:ZnS crystal, that could operate at up to 5 W of Er:fiber pump, delivering in CW regime up to 1.2 W of output power with 19% output coupler. In a 1 m long cavity with 145 MHz repetition rate the laser [106] generated high spectral and spatial quality near transform-limited pulses of only 69 fs in duration at 3.8 nJ pulse energy, 145 MHz repetition rate and 550 mW average output power (see Fig. 18).

Dispersion compensation was achieved with a single 1 mm sapphire plate and a single bounce from the chirped mirror. This was possible owing to the shorter active element and almost twice lower dispersion of ZnS than in ZnSe (2.5 mm and 123 fs^2 vs. 4 mm and 220 fs^2, respectively). As a positive side effect, the third order dispersion decreases as well, allowing to reach even shorter pulse duration as we shall show later. Further increasing the pump power up to 1 W resulted in double-pulse regime, with the pulse energy effectively limited to the same 3.8 nJ level. Inside the cavity this corresponded to 20 nJ, and beyond this value the nonlinearity in the active medium caused the pulse break-up. Some improvement to this limit was achieved in a shorter cavity (bigger mode volume), with up to 1 W of output power at 210 MHz repetition rate, corresponding to 4.7 nJ energy [36] at the expense of somewhat longer pulse duration of 75 fs.

Another option to overcome this limit, is to provide higher outcoupling rate, e.g. using the broadband 20% output coupler in a folding mode, bringing the effective output transmission to 35% [107]. This brings the maximum output power to 820 mW (7.8 nJ pulse energy) in single-pulse regime. Fig. 19 summarizes the results.

It is important to note that all experiments were performed at room temperature, without active cooling. With proper thermal management and more pump power, higher average power seems feasible.

B. Chirped-Pulse Cr:ZnS Laser

Increasing the energy beyond the pulse break-up limit, set by the excess self-phase modulation in the active medium, is possible by operating the laser in the positive (normal) dispersion regime. In this case the propagating pulse acquires strong chirp and is extended in time. This regime is called a dissipative soliton or, by analogy to chirped-pulse amplifier, a chirped-pulse oscillator (CPO). This regime, first studied as a side effect [81], [82], [108] has been put on a solid theoretical basis [109]–[111] and has now become an accepted and commercially successful approach to scale up the pulse energies of solid-state oscillators.

The important property of these oscillators is the possibility to dechirp the output pulse by a simple dispersion stage providing negative (anomalous) group delay dispersion, such as e.g. a prism pair, back to the femtosecond domain to regain the peak intensity required by the applications. Our simulations based on the analytical theory presented in [111] predict feasibility to scale the pulse energy in the femtosecond Cr:ZnSe and Cr:ZnS oscillators up to μJ levels [112], [113]. In what follows we describe our experiments towards implementation of this ambitious goal.

The first observation of the CPO regime in a Cr:ZnSe oscillator occurred in a KLM laser [104], operated under high third-order dispersion near the dispersion zero crossing. The laser was able to spontaneously switch the operation wavelength to the chaotic [105], [114], [115] CPO regime. The CPO regime has also been demonstrated in the SESAM-modelocked Cr:ZnS and Cr:ZnSe lasers [100], but as the output parameters were mostly limited by the SESAM, the achieved energy did not exceed 1.1 nJ in the best case.

Much better results could be demonstrated using the KLM setup, where the positive dispersion regime allowed reaching the 8.4 nJ output energy at 105 MHz (see Fig. 20) and pulse durations from 0.8 to 2 ps with nearly rectangular 100-nm broad spectra [107]. Most importantly, the energy scaling was achieved in a low-output configuration, in which the soliton laser output energy was limited to 3.8 nJ by the pulse break-up. In the CPO configuration, the laser operated in a reliably single pulse mode across the wide range of pump powers, adapting to higher energy by increasing chirp. Thus it becomes possible to reach even higher pulse energies in the longer resonators.

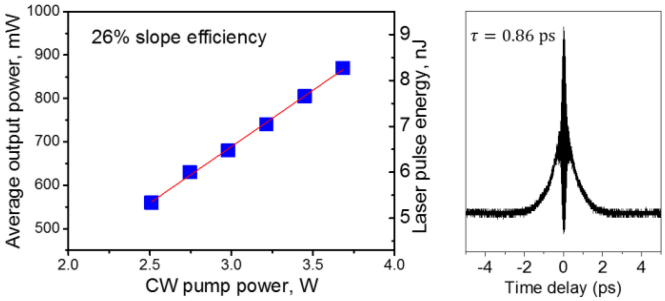

Fig. 20. Output characteristics of a chirped-pulse KLM Cr:ZnS oscillator (left) and a typical autocorrelation trace [107].

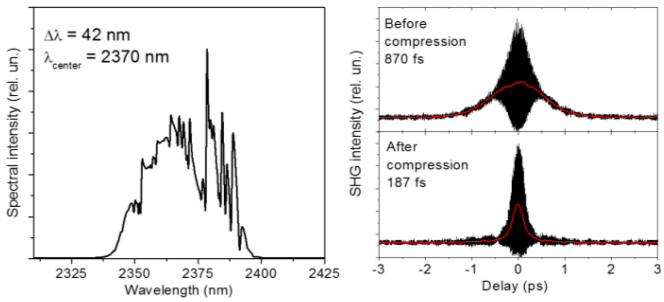

Fig. 21. (*Left*) Spectrum of the graphene mode-locked Cr:ZnS chirped pulse oscillator with extended cavity. The high-frequency modulation is due to the intracavity water vapor absorption in the atmosphere [17]. (*Right*) Pulse autocorrelation traces before and after compression.

This has been demonstrated in [116] and [117], where we realized the first high-energy graphene mode-locked Cr:ZnS laser operating in the positive dispersion regime. Extending the resonator round-trip length to 6.5 m, we obtained pulses with 15.5 nJ energy and 42 nm spectral bandwidth with 0.87 ps duration (see Fig. 21). The chirp could be compressed with a simple two-prism compressor at 60 cm distance down to 187 fs (see Fig. 21, right). The graphene SA provided reliable self-starting within 0.5 ms after interruption, but also turned to be the weak point of the setup. The very fast relaxation times of graphene (<0.2 and 1.5 ps [118], [119]), which are shorter or comparable to the pulse duration, result in a very high thermal load onto the graphene layer, causing its irreparable damage, if the focusing spot is too small [116].

C. Few-Cycle Graphene and CNT Mode-Locking

The advance of graphene and carbon nanotube (CNT) saturable absorbers for mode-locking in the recent years came as a real break-through to the infrared mode-locked laser technology. A major advantage of these materials is that they have very broadband saturable absorption, and allow deposition techniques compatible with most optical materials. With saturation fluences of tens of μJ/cm^2 and double decay time of 100–200 fs and ~1.5 ps for intraband electron scattering and optical phonon cooling, respectively [119] graphene is a convenient and extremely fast saturable absorber, with nearly uniform spectral response from the visible to the infrared. Parameters of the

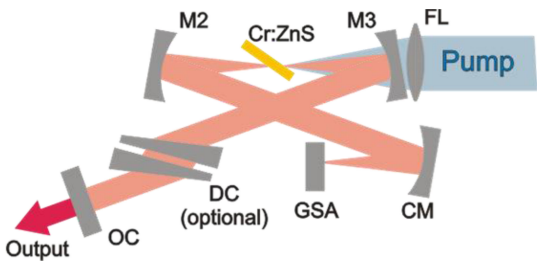

Fig. 22. Experimental setup of the graphene mode-locked Cr:ZnS laser [124], [125]. FL: Pump focusing lens, CM: Chirped mirror, GSA: Graphene-based saturable absorber mirror, OC:output coupler, DC: Dispersion compensation.

CNT saturable absorbers vary upon manufacturing and deposition process; their size-dependent absorption bands are typically located below 2 μm. A compilation of mode-locked laser demonstrations can be found in [120], and new results keep arriving almost on a monthly basis.

Graphene mode-locking has been first demonstrated in Cr:ZnSe [121], [122], using a single graphene layer deposited on a CaF_2 plate, positioned at Brewster angle in an additional resonator focus. With a CaF_2 prism pair for dispersion compensation, the Tm:fiber laser pumped setup produced up to 185 mW of output power with pulse duration between 176 and 200 fs [122]. At 78 MHz repetition rate, the 2.4 nJ output energy is so far the highest pulse energy, obtained from a Cr:ZnSe-based laser. Recently, a graphene-gold saturable absorber (GSA) was used to demonstrate a tunable femtosecond Cr:ZnSe laser [123].

Much higher energy and shorter pulses could be demonstrated with a Cr:ZnS active medium using a reflection-type saturable absorber, with graphene single and double layers deposited directly onto the high reflector end mirror of the resonator (see Fig. 22). Dispersion compensation was achieved by two bounces from the focusing chirped mirror and could additionally by adjusted by thin YAG wedges at Brewster angle.

A Cr:ZnS laser with this kind of GSA showed remarkable reliability in self-starting within few 100 μs after opening the cavity and flexibility in resonator configurations. The output power reached 250 mW level at 108 MHz repetition rate in single pulse regime, corresponding to 2.3 nJ pulse energy at 49 fs pulse duration. Higher output power up to 815 mW was possible, but only in the multipulsing regime. Even shorter pulse duration of 41 fs was obtained with a 1.8% output coupler with 75 mW output power (see Fig. 23). At such short duration, the pulse spectrum fills most of the water-free atmospheric window and some dry air purging became necessary. The achieved 41 fs pulse duration corresponds to only five optical cycles of the electric field. These are now the shortest pulses ever generated from any laser in the mid-infrared wavelength range above 1.5 μm. Combined with the demonstrated power-handling capability and self-starting, the GSA technology seems to be the most appropriate for applications.

A CNT saturable absorber mirror has also proved a feasible alternative to mode-lock a Cr:ZnS laser [126]. The 80-μm thick CNT layer was essentially single-walled with diameter 1.2–1.8 nm, measured initial absorption of 5.1%, and saturation

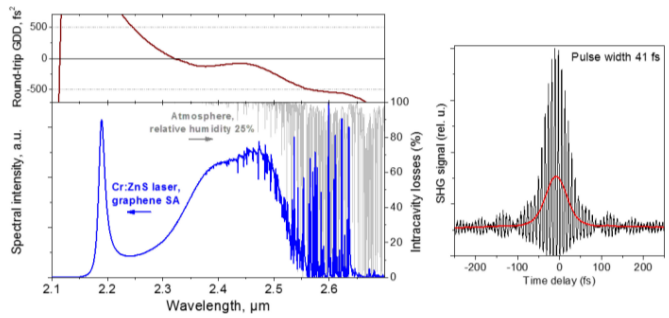

Fig. 23. Few-cycle Cr:ZnS laser. *Left graph:* Output spectrum (blue), calculated round-trip GDD (dark red). *Right graph:* Fringe-resolved (black) and intensity autocorrelation trace (red). Adapted from [124].

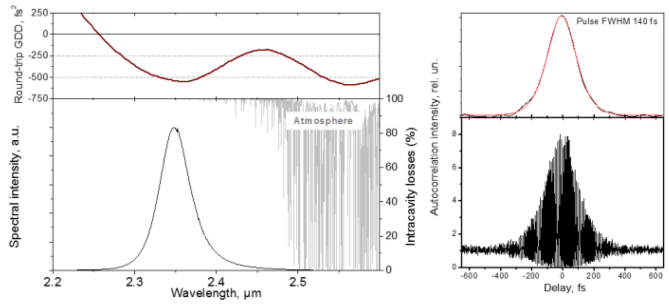

Fig. 24. High-power ceramic Cr:ZnS laser. *Left graph:* Output spectrum (blue), calculated round-trip GDD (dark red). *Right graph:* Fringe-resolved (black) and intensity autocorrelation trace (red). Adapted from [127].

fluence about three times higher than for graphene mirror. The CNT saturable absorber was able to support mode-locked operation indefinitely long, but required slight initial perturbation to start the pulsed regime. It was also more sensitive to overheating, which resulted in most cases in irreparable spot damage. With a short cavity at 250 MHz repetition rate the laser emitted 950 mW of average output power (3.8 nJ pulse energy) with 61 fs duration [126] – so far the shortest pulses produced from any CNT mode-locked laser.

D. High-Power Ceramic Cr:ZnS Oscillator

Graphene saturable absorber also proved very useful in providing reliable high-power mode-locking of a laser based on ceramic Cr:ZnS material [127]. The setup utilized a short, 270 MHz cavity and increased negative group delay dispersion, providing up to 1.05 W of average output power (3.8 nJ energy) with 140 fs pulse duration (see Fig. 24).

As compared to the single-crystal based setup described previously, this experiment utilized shorter active element, causing the group-delay dispersion to be overcompensated at -500 fs^2. The resulting pulse duration of 140 fs is therefore not optimal and subject to optimization.

The presented result clearly outperforms not only the SESAM-based lasers described in Section IV-B. It also generates over an order of magnitude higher output power and about 8 times higher energy than the recently published Kerr-Lens mode-locked Cr:ZnS and Cr:ZnSe polycrystalline lasers [99] at comparable pulse duration.

E. Summary of Results

Table I summarizes the demonstrated femtosecond and chirped-pulse Cr^{2+}-based lasers discussed in the previous sections. Note that for every configuration we quote the highest output power and energy, the shortest pulse duration (FWHM) and the broadest spectral width (FWHM), which may have not been obtained simultaneously, or improved after publication.

VI. Applications

The main advantage, offered by the Cr^{2+}-based ultrafast lasers is undoubtedly their unique operation wavelength range. Therefore, those applications will benefit the most, which critically depend on this property. A good example is molecular spectroscopy, where it becomes possible to address directly the fundamental vibrational frequencies or low-order overtones, thus gaining orders of magnitude in sensitivity as compared to the near-infrared sources. Another case in point is pumping the nonlinear-optical materials, which wouldn't operate at shorter wavelengths, but are very efficient in the mid-IR. At the same time, the mid-IR wavelength region imposes certain constraints, like e.g. strong absorption of the atmosphere. In what follows we shall describe those applications that have already been demonstrated and discuss possibilities that are opening with the recent advances in high-power femtosecond generation in Cr^{2+}-based media.

A. Femtosecond Lasers for Molecular Spectroscopy

A femtosecond laser can be used in high-resolution spectroscopy in various ways, see e.g. reviews [13], [128]–[130]. Even the most simple and straightforward way such as using the laser as an illumination source in combination with a conventional spectrometer, brings enormous advantage as compared to the traditional incoherent (e.g. thermal) broadband source. The unique property of femtosecond and supercontinuum sources is the combination of a broad spectrum with the perfect transversal coherence, allowing reaching brilliance orders of magnitude higher than any other source of broadband radiation smaller than a synchrotron. Spectroscopy of most gas molecules requires resolution of $\Delta\nu \sim 0.1$ cm^{-1} (typical linewidth in the atmosphere at normal conditions) or better. To achieve this resolution using an incoherent source would require reducing the throughput of a spectral device, e.g. by selecting the Jaquinot stop throughput in a FT spectrometer (FTIR) proportionally to the required resolution: $S \propto \Delta\nu$. With the noise-limited performance, this makes the signal-to-noise ratio (SNR) proportional to the resolution, and the recording time required to reach a given SNR thus scales quadratically with the inverse resolution $T \propto \Delta\nu^{-2}$. Using a coherent, diffraction-limited beam allows using the maximum throughput *independently* from the required resolution. In this sense, the advantage of the laser sources, which is already significant given their higher spectral power density, additionally grows quadratically with improving resolution.

TABLE I
ULTRASHORT-PULSED Cr^{2+}-BASED LASERS

Active medium	Crystal type	Pump source	Mode-locking mechanism	Dispersion compensation	P_{out} (mW)	E_{out} (nJ)	$\Delta\tau$ (fs)	$\Delta\lambda$ (nm)	λ_0 (nm)	References
Cr:ZnSe	NS	NaCl:OH^-	AOM	no	82	0.38	4400	2.2	2470	[77]
	single	Co:MgF_2	AOM	no	400	4	4300–30000		~2500	[25]
	NS	Tm:YALO	SESAM	no	400	3.3	10800	0.75	~2500	[85]
	single	Er:fiber	SESAM	no	140	0.93	970	~20	~2450	[86]
			SESAM	sapphire	75	0.38	100	60	2450	[26]
			SESAM	CM + YAG	80	0.44	80	105	2420	[87]
			SESAM	CM + sapphire	90	0.5	132	47	2420	[100]
			SESAM, CPO	CM + YAG	100	0.55	730	69	2370	[100]
			KLM	YAG	300	3	100	72	2500	[104]
			KLM, CPO	YAG	170	1.7	1000	70	2350	[104]
	NS	Tm:fiber	KLM	YAG	41	0.45	116	69	2427–2450	[72]
			KLM	CaF_2 prisms	165	1.81	92	76	2451–2459	[72]
			KLM	MgF_2 prisms	40	0.4	95	69	2421	[72], [103]
			graphene	CaF_2 prisms	185	2.4	176	43	2400, 2500	[121], [122]
	poly	Er:fiber	SESAM	sapphire	100	0.47	100	70	2450	[89]
			KLM	YAG + FS	60, 250[a]	0.5, 1.5[a]	100	75	2400	[99]
	NS	Er:fiber	graphene	CaF_2 prisms	66	0.67	116	50	2310–2426[b]	[123]
Cr:ZnS	single	Er:fiber	SESAM	no	125	0.83	1100	~10	2450	[86]
			SESAM	CM + YAG	130	0.72	130	48	2375	[90], [100]
			SESAM, CPO	CM	205	1.14	630	102	2410	[90], [100]
			KLM	CM + sapphire	1000	7.8	69	91	2390	[36], [106], [107]
			KLM, CPO	CM + YAG	880	8.2	800–2000	150	2350	[105], [107]
			graphene	CM + YAG	815	2.3	41	190	2400	[124], [125]
			graphene, CPO	CM + YAG	890	15.5	870–1200, 189[c]	65	2350–2450	[116]
			CNT	CM	950	3.8	61	85	2350	[126]
	poly	Er:fiber	SESAM	sapphire	120	0.67	116	50	2390	[90]
			KLM	YAG + FS	30	0.25	125	45	2350	[99]
			graphene	CM	1050	3.9	140	45	2349	[127]

AOM: Acousto-optic modulator; CM: Chirped mirror; NS: Not specified; CPO: Chirped-pulse oscillator; FS: Fused silica.
[a] With extracavity amplification. [b] Tunable. [c] After extracavity compression.

This approach has been first realized with a femtosecond OPO at 3.5 μm [8], [131]. The simple home-made FTIR arrangement and several mW of the idler OPO beam allowed reaching only 2.6 cm^{-1} resolution, but demonstrated feasibility of the technique. Shortly after the first femtosecond Cr:ZnSe laser had been developed, it was used to record spectra with 0.125 cm^{-1} resolution within 13 s and with 3800 SNR [10]. The experiment utilized a commercial FTIR spectrometer, a single-pass 70-cm gas cell, and a femtosecond Cr:ZnSe laser at 200 MHz repetition rate (see Fig. 25).

The laser has been put into an evacuated chamber that contained water-free gas mixture guaranteeing that the output spectrum is free of the intracavity absorption signal (see Section III). This, in turn, required that the laser should be reliably self-starting, which was provided by the SESAM structure. Fig. 26 shows the output spectra before and after the acetylene gas cell, as well as the retrieved absorption signal.

In the setup, the complete spectrum could be recorded within only 13 s, set by the FTIR mechanics at maximum resolution. The observed SNR ratio reached 3800, despite the fact that the 70 mW signal had to be attenuated by about 100 times in order to stay within the safe limits of the detector. This clearly shows the potential of the technique, which can tolerate significant beam attenuation e.g. in a remote sensing mode or within a multipass cell.

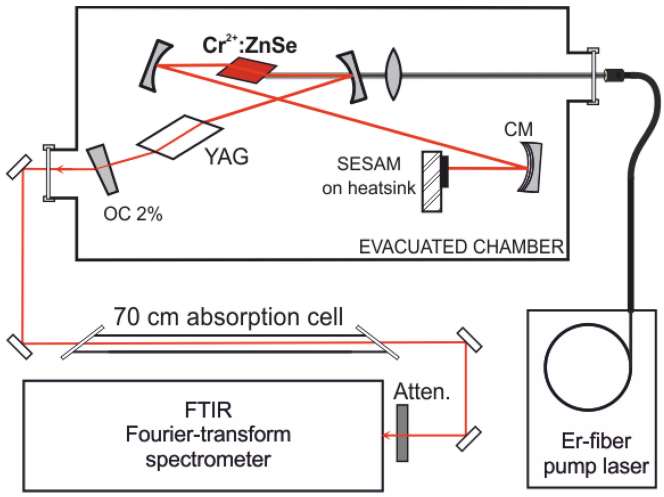

Fig. 25. Experimental setup for high-resolution mid-IR molecular spectroscopy (adapted from [10]). CM: Chirped mirror.

B. Dual-Comb Spectroscopy

The radical shortening of the recording time can be reached by eliminating the slowest part of the setup—the mechanical FTIR spectrometer. This can be done by using a second femtosecond laser operating at the slightly different pulse repetition

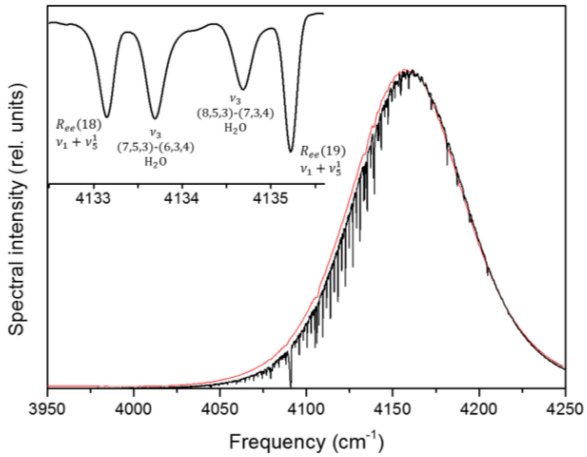

Fig. 26. Acetylene absorption measurement (adapted from [10]). Red: Pulse spectrum (baseline), black – spectrum after acetylene cell propagation. Inset shows the detail of the retrieved spectrum with spectral line designations.

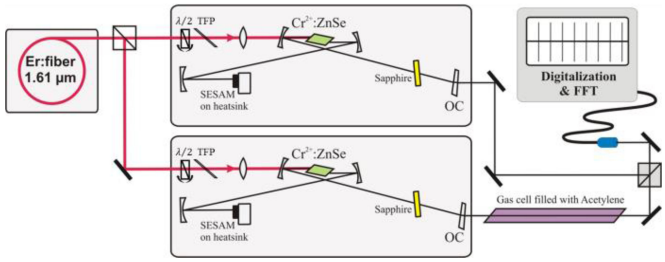

Fig. 27. Dual-comb setup at 2.4 μm (adapted from [13]). TFP: Thin-film polarizer.

rate, the dual-comb approach. This method, originally suggested in 2004 [11] uses cross-correlation signal provided by the interfering pulse sequences to obtain complete Fourier spectra at a rate, equal to the repetition rate difference between the two lasers, typically few hundreds spectra per second, allowing spectroscopic recording of transient processes [132]. The dual-comb spectroscopy has a natural application focus in the mid-IR. Originally demonstrated with a difference frequency generation [11], [132], it has been extended to include OPOs [133] and coherent Raman interaction [134]. Cr^{2+}-based lasers allow bringing the dual-comb spectroscopy directly to the mid-IR in a most straightforward way. The feasibility of such application has been demonstrated with the Cr:ZnSe femtosecond lasers [13].

The experimental setup included two identical Cr:ZnSe laser based on ceramic materials [89], pumped by a single Er-fiber laser, providing up to 2 W finely controllable power in two channels (see Fig. 27). The lasers were made transportable with a footprint of 30×60 cm each and operated at 200 MHz repetition rate with about 400 Hz difference. The interference signal was recorded with a fast extended-InGaAs detector. All equipment operated at room temperature. With a sample cell in one arm (see Fig. 27) it was possible to obtain the first proof-of-principle spectra of the acetylene $\nu_1 + \nu_5^1$ band (see Fig. 28). Taking the 10 μs burst length for the fast FT, 0.4 cm^{-1} resolution in the

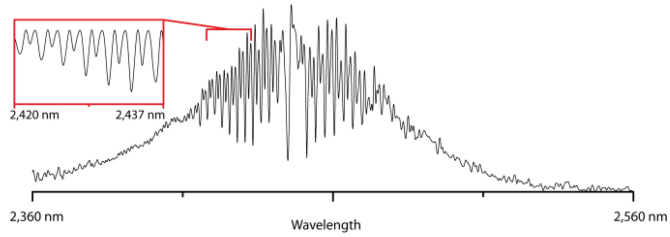

Fig. 28. Acetylene spectrum, obtained from a single burst [13].

optical domain can be obtained, sufficient for clear identification of the species in the sample and its concentration measurement. Such spectra can be recorded every 2.5 ms.

C. *Intracavity Absorption and Protected Delivery*

The mid-IR spectral range, being very promising for spectroscopic applications, itself represents a challenge, because the atmosphere is not completely transparent anymore. Water vapor absorption lines are present almost everywhere, except the 2.1–2.4 window. This leaves only a relatively narrow operation range. For all other wavelengths water absorption lines represent an issue to be dealt with. The effect of the molecular absorption lines turns out to be tremendously different when the absorption takes place inside the cavity. The reason for this is that pulse propagation in a femtosecond oscillator is nonlinear. In comparison to linear propagation through the atmosphere or a gas cell outside of the cavity, where absorption line causes a narrow dip in the spectrum, the nonlinear interaction continuously fills the spectral gap. At the same time the nonlinearity causes phase delay of the pulse with respect the phase velocity of a linear wave. The narrowband absorption feature in time domain is a long tail behind the pulse, with negligible overlap with the high-intensity pulse. Therefore, the tail propagates as a linear wave, and accumulates phase difference with the pulse itself. The analytical description of this process [92], [135] stipulates that the steady-state solution occurs when phase delay reaches 90°, so that the absorption line becomes a dispersion-like feature (blue line in Fig. 29).

In addition to the predictable shape, the intracavity absorption signal has also a well-defined amplitude, which can be calculated using the design and observable parameters such as the dispersion and spectrum width [92]. This amplitude is typically an order of magnitude higher than in the corresponding extracavity signal in a cell with the length equal to the round-trip length of the laser resonator. This is clearly seen in Fig. 29, where the amplitude of the blue signal is comparable to the grey signal, while the absorbing gas concentration is 17 times lower.

The enhancement of the intracavity absorption signal can be further increased in the CPO. The analytical theory [135] predicts that while the intracavity absorption signal near the spectrum center is comparable to that for the conventional (soliton) laser, there is an additional strong enhancement near the spectral edges. Experimental observation using a Cr:ZnS laser have demonstrated a 140-fold enhancement of the absorption signal [138]. Fig. 30 compares the water vapor absorption over the

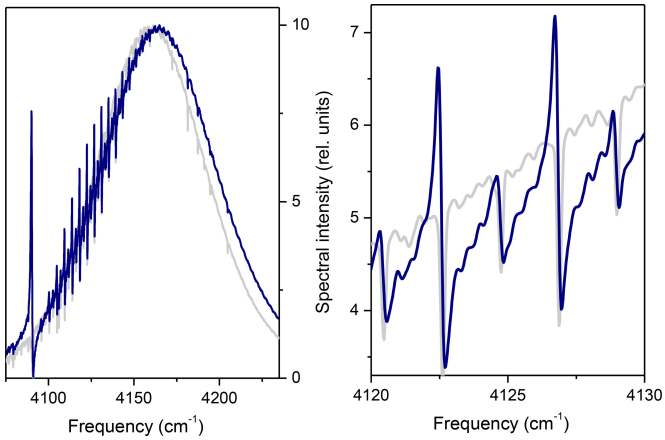

Fig. 29. Comparison of the extra-cavity (gray, 17 mbar acetylene, path 70 cm) and intracavity (blue, 1 mbar acetylene, round-trip path 150 cm) absorption signals with a femtosecond Cr:ZnSe laser [136], [137].

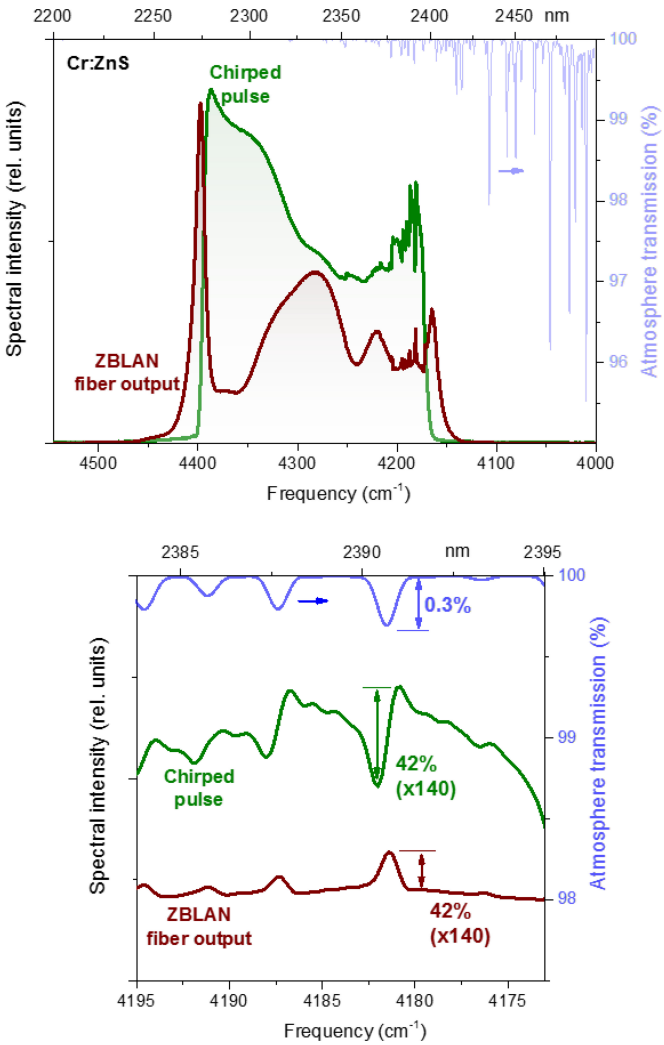

Fig. 30. Intracavity absorption in chirped-pulse Cr:ZnS laser (green curve). The lower graph shows the expanded view of the spectrum edge. The dark red signal is the spectrum after propagation in 2 m of ZBLAN fiber.

round-trip (blue) with the laser output spectrum (green), demonstrating the near-edge enhancement. The dark red signal shows the spectrum after propagation the 2 nJ pulse in a ZBLAN fiber. After initial chirp compensation, the high energy of the pulse is sufficient to initiate soliton fission, again resulting in accumulation of an additional phase delay with respect to the narrowband tail. The result is the conversion of the dispersion-like signal to a more familiar peak-type signal (phase delay $-200°$) as seen in the lower graph.

Thus, the intracavity absorption in a femtosecond laser does not prevent operation, and can even be useful for spectroscopic and sensing purposes. However, if the laser is going to be used as a source for spectral measurements, the narrowband modulation due to the atmospheric absorption is not desired. While the laser itself can be protected, like e.g. in Fig. 25, there still remains an issue of beam delivery to the object. This can be solved by an optical fiber, which do exist for this spectral region, however, the propagation becomes necessarily nonlinear. Luckily, the typical and commercially available ZBLAN fiber, offering transparency between 2 and 3 μm also has a reduced nonlinearity and a fairly flat anomalous dispersion curve. This allows propagating pulses form Cr:ZnSe and Cr:ZnS with typical durations and energies through a single-mode ZBLAN fiber close to the soliton regime, i.e. maintaining the pulse temporal and spectral width [139]. Fig. 31(a) and (b) show the output spectra at different launched energies. It is evident that the spectrum gets somewhat narrower at energy corresponding to half of the fundamental soliton($N = 0.5$) and then restores it original width at $N = 1$ energy. At this point the output pulse width becomes equal to the launched [see Fig. 31(c) and (d)], i.e. the pulse propagates practically undisturbed. Some spectrum shift which is observed on the experimental trace [see Fig. 31(b)] is obviously due to the Raman interaction, which was not included into the simulation. For shorter pulses the launched energy will be higher, according to the soliton area theorem $E \cdot \tau = 2|\beta_2|/\gamma$, but still lies close to the typical parameters, described in the previous sections.

D. Mid-IR Parametric Oscillators

Besides spectroscopic applications, high energy femtosecond Cr:ZnSe and Cr:ZnS lasers are interesting as pump sources for nonlinear optical conversion, especially in combination with materials, which cannot operate with other, shorter-wavelength femtosecond oscillators. A good example is the orientation patterned GaAs (OP-GaAs)—an analogue to the periodically poled nonlinear crystals, allowing quasi-phase matched operation and possessing a number of special properties, such as very high nonlinear coefficient $d_{14} = 94$ pm/V and extended transparency region up to 17 μm [140]. This material cannot be pumped with available Ti:sapphire, Yb- or Er-doped femtosecond oscillators because of direct or two-photon absorption. Using the OP-GaAs would have required therefore an additional OPO stage [141] with the corresponding loss of performance and cost increase. With Cr:ZnSe pump source, OP-GaAs has

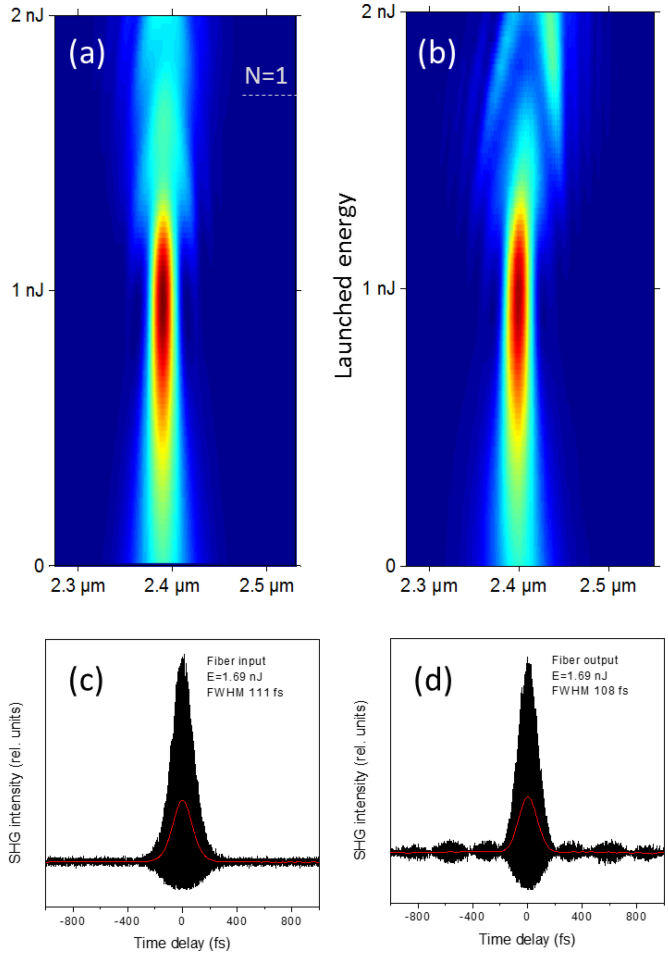

Fig. 31. Propagation of a 110-fs pulse in ZBLAN fiber. Simulated (a) and experimental (b) output spectra at different launched pulse energy. Input (c) and output (d) autocorrelation traces at $N = 1$ soliton energy. Adapted from [139].

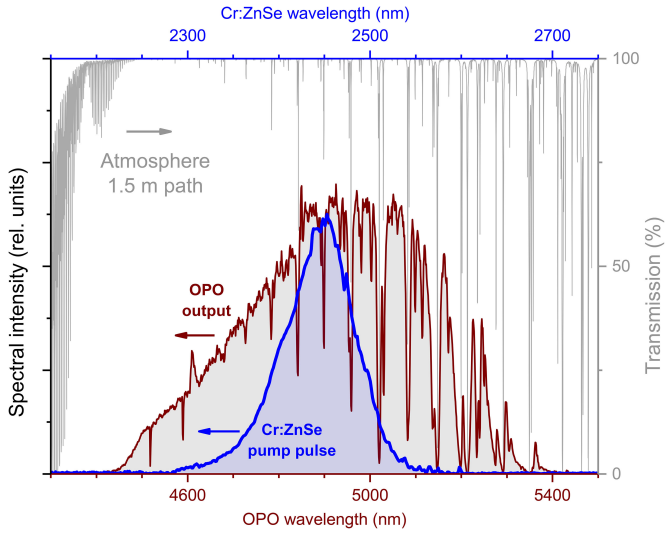

Fig. 32. Output spectrum (dark red) of an OP-GaAs subharmonic OPO, pumped by a Cr:ZnSe laser (blue). The atmospheric absorption (right Y-scale) significantly modifies the OPO spectrum.

been shown to generate broadband radiation between 4.5 and 5.4 μm [142].

The experimental setup used synchronous pumping by the 182-MHz Cr:ZnSe laser with pulses about 100 fs duration centered at 2.45 μm (blue spectrum in Fig. 32). The average power at the OPO input was limited to 100 mw or 0.55 nJ pulse energy, which was focused by a 50-mm r.o.c. mirror on the OP-GaAs sample. The 0.5-mm thick OP-GaAs device had only 5 domain reversal periods of 92 μm thickness, thus allowing quite broadband gain. With a pump threshold at 60 mW (0.33 nJ), the OPO delivered broadband output spectrum (dark red in Fig. 32), almost completely filling the transparency region between the CO_2 band at 4.3 μm and the water absorption band above 5.5 μm. It is worth noting, that the spectral width of the OPO depends mostly on the dispersion and available pump [143], [144], and already in this experiment exceeded that of the Cr:ZnSe laser. With the recent advances in high-energy, short pulse Cr:ZnS oscillators like described above, the subharmonic OPO will become even more efficient and versatile, opening way to practical applications of such sources.

VII. Conclusion

Cr^{2+}- based femtosecond lasers—notably Cr^{2+}:ZnSe and Cr^{2+}:ZnS—have come of age. In particular, Cr^{2+}:ZnS can be truly called now "Ti:sapphire of the mid-infrared". Both, in single crystalline as well as ceramic form, Cr^{2+}:ZnS lasers now produce exceptionally stable low frequency noise near transform-limited pulses – frequency combs - with a pulse duration down to five optical cycles (~40 fs) at Watt-level output powers and tens of nanojoule pulse energies directly from the oscillator. The good power handling capabilities of Cr^{2+}:ZnS together with the smaller than in Ti:sapphire Stokes shift makes this material comparable to Yb:YAG in terms of power scaling. Future improvements of the thin-disk and CPO designs in a master oscillator power amplifier geometry will be the way forward to obtain high powers and high energies from these lasers, which makes them particularly attractive for efficient X-Ray generation as well as for a multitude of industrial applications.

As such, these compact and robust fiber-laser pumped femtosecond mid-IR sources are perfect tools for ultraprecise and ultrasensitive spectroscopy, with sensitivities that reach well into the ppb or even the ppt range. Advanced realizations of such spectroscopic devices include, but are not limited to a frequency comb FT spectrometer as well as a dual-comb spectrometer. The latter device represents a leap forward in modern spectroscopic techniques as it allows reaching virtually unlimited resolution and ms recording speeds. One of the immediate applications would be hydrocarbon detection and chemical fingerprinting of oil and oil related trace gases. Another obvious use is breath analysis. The unprecedented sensitivity offered by femtosecond sources in this wavelength region allows for the monitoring and early prediction of various human diseases, which includes early cancer recognition. The same laser features, which are attractive for sensor applications, namely, the possibility to

adjust the wavelength of the laser to the desirable absorption band, make these lasers desirable tools also for fine surgery of biologic tissue, e.g. in ophthalmology and brain surgery.

Looking into the future, one may envisage engineered ceramic Cr^{2+}-laser materials with desirable laser and nonlinear properties. This will allow, for example, the practical use of the effect of simultaneous generation of two phase matched frequency combs in one and the same laser, one at the fundamental frequency and one at second harmonic that we recently observed. Such a "double pulse" femtosecond comb source might become compact and cost-effective frequency transfer device for precision metrology and transportable optical frequency standards.

Note Added in Proof: Dramatic improvements of laser parameters listed in Table I have been achieved since the final revision of this paper. In particular, a GHz-class femtosecond Cr:ZnS with up to 0.8 W of output power at 0.96 GHz repetition rate has been demonstrated in out group and is due to be reported at ASSL 2014 conference. At CLEO 2014 the authors of Ref. [99] reported a Kerr-lens mode-locked ceramic Cr:ZnS laser with up to 2 W of output power and up to 0.25 W of intracavity SHG.

ACKNOWLEDGMENT

The authors would like to thank the invaluable input over the years of their collaborators and colleagues: G. Guelachvili, A. Di Lieto, V. Kalashnikov, N. Kuleshov, V. Levchenko, J. Mandon, S. Mirov, R. Page, N. Picqué, K. Schaffers, N. Tolstik, M. Tonelli, E. Vinogradov, and K. Vodopyanov.

REFERENCES

[1] I. T. Sorokina, "Broadband mid-infrared solid-state lasers," in *Mid-Infrared Coherent Sources and Applications*, M. Ebrahim-Zadeh and I. T. Sorokina, Eds. New York, NY, USA: Springer, 2008, pp. 225–260.

[2] C. Fischer, E. Sorokin, T. Sorokina, and M. Sigrist, "Photoacoustic gas spectroscopy using a tunable solid state laser emitting around 2.4 μm," presented at the Conf. Lasers Electro-Opt./Int. Quantum Electron. Conf., San Francisco, CA, USA, 2004, Paper CMN5.

[3] E. Sorokin, I. T. Sorokina, C. Fischer, and M. W. Sigrist, "Widely tunable Cr^{2+}:ZnSe laser source for trace-gas sensing," in *Proc. Adv. Solid-State Photon.*, 2005, pp. 826–830.

[4] E. Sorokin, "Ultrabroadband solid-state lasers in trace gas sensing," in *Mid-Infrared Coherent Sources and Applications*, M. Ebrahim-Zadeh and I. T. Sorokina, Eds. New York, NY, USA: Springer, 2008, pp. 557–574.

[5] N. Tolstik, E. Sorokin, V. Kalashnikov, D. Klimentov, V. Dvoyrin, and I. T. Sorokina, "Supercontinuum generation in mid-IR using chalcogenide and germanate nonlinear fibers," *Proc. SPIE*, vol. 8599, p. 85990K, 2013.

[6] N. Tolstik, E. Sorokin, and I. T. Sorokina, "Supercontinuum generation in mid-IR using chalcogenide nonlinear fiber," presented at the 50 Years Nonlinear Opt., Barcelona, Spain, 2012, p. TP–NT.

[7] S. Schiller, "Spectrometry with frequency combs," *Opt. Lett.*, vol. 27, pp. 766–768, 2002.

[8] K. A. Tillman, R. R. J. Maier, D. T. Reid, and E. D. McNaghten, "Mid-infrared absorption spectroscopy of methane using a broadband femtosecond optical parametric oscillator based on aperiodically poled lithium niobate," *J. Opt. A, Pure Appl. Opt.*, vol. 7, pp. S408–S414, 2005.

[9] J. Mandon, G. Guelachvili, N. Picqué, F. Druon, and P. Georges, "Femtosecond laser Fourier transform absorption spectroscopy," *Opt. Lett.*, vol. 32, pp. 1677–1679, 2007.

[10] E. Sorokin, I. T. Sorokina, J. Mandon, G. Guelachvili, and N. Picque, "Sensitive multiplex spectroscopy in the molecular fingerprint 2.4 μm region with a Cr^{2+}:ZnSe femtosecond laser," *Opt. Exp.*, vol. 15, pp. 16540–16545, Dec. 10, 2007.

[11] F. Keilmann, C. Gohle, and R. Holzwarth, "Time-domain mid-infrared frequency-comb spectrometer," *Opt. Lett.*, vol. 29, pp. 1542–1544, 2004.

[12] I. Coddington, W. Swann, and N. Newbury, "Coherent multiheterodyne spectroscopy using stabilized optical frequency combs," *Phys. Rev. Lett.*, vol. 100, p. 013902, 2008.

[13] B. Bernhardt, E. Sorokin, P. Jacquet, R. Thon, T. Becker, I. T. Sorokina, N. Picqué, and T. W. Hänsch, "Mid-infrared dual-comb spectroscopy with 2.4 μm Cr^{2+}:ZnSe femtosecond lasers," *Appl. Phys. B*, vol. 100, pp. 3–8, 2010.

[14] H. Xiong, H. Xu, Y. Fu, J. Yao, B. Zeng, W. Chu, Y. Cheng, Z. Xu, E. J. Takahashi, K. Midorikawa, X. Liu, and J. Chen, "Generation of a coherent x ray in the water window region at 1 kHz repetition rate using a mid-infrared pump source," *Opt. Lett.*, vol. 34, pp. 1747–1749, Jun. 1, 2009.

[15] T. Popmintchev, M. C. Chen, D. Popmintchev, P. Arpin, S. Brown, S. Alisauskas, G. Andriukaitis, T. Balciunas, O. D. Mucke, A. Pugzlys, A. Baltuska, B. Shim, S. E. Schrauth, A. Gaeta, C. Hernandez-Garcia, L. Plaja, A. Becker, A. Jaron-Becker, M. M. Murnane, and H. C. Kapteyn, "Bright coherent ultrahigh harmonics in the keV x-ray regime from mid-infrared femtosecond lasers," *Science*, vol. 336, pp. 1287–91, Jun. 8, 2012.

[16] R. H. Page, L. D. DeLoach, G. D. Wilke, S. A. Payne, and W. F. Krupke, "A new class of tunable mid-IR lasers based on Cr^{2+}-doped II-VI compounds," presented at the Conf. Lasers Electro-Opt., Baltimore, MD, USA, 1995, Paper CWH5.

[17] L. D. DeLoach, R. H. Page, G. D. Wilke, S. A. Payne, and W. F. Krupke, "Properties of transition metal-doped zinc chalcogenide crystals for tunable IR laser radiation," presented at the Adv. Solid State Lasers, Memphis, TN, USA, 1995, Paper LM4.

[18] R. H. Page, K. I. Schaffers, L. D. Deloach, G. D. Wilke, F. D. Patel, J. B. Tassano, Jr., S. A. Payne, W. F. Krupke, K. T. Chen, and A. Burger, "Cr^{2+}-doped zinc chalcogenides as efficient, widely tunable mid-infrared lasers," *IEEE J. Quantum Electron.*, vol. 33, no. 4, pp. 609–617, Apr. 1997.

[19] L. D. DeLoach, R. H. Page, G. D. Wilke, S. A. Payne, and W. F. Krupke, "Transition metal-doped zinc chalcogenides: Spectroscopy and laser demonstration of a new class of gain media," *IEEE J. Quantum Electron.*, vol. 32, no. 6, pp. 885–895, Jun. 1996.

[20] R. H. Page, L. D. DeLoach, G. D. Wilke, S. A. Payne, R. J. Beach, and W. F. Krupke, "Cr^{2+}-doped II-VI crystals: New widely-tunable, room-temperature mid-IR lasers," in Proc. IEEE Lasers Electro-Opt. Soc. Ann. Meet.. 8th Ann. Meet. Conf., 1995, vol. 2, pp. 449–450.

[21] G. J. Wagner, T. J. Carrig, R. H. Page, K. I. Schaffers, J.-O. Ndap, X. Ma, and A. Burger, "Continuous-wave broadly tunable Cr^{2+}:ZnSe laser," *Opt. Lett.*, vol. 24, pp. 19–21, Jun. 1, 1999.

[22] I. T. Sorokina, E. Sorokin, A. D. Lieto, M. Tonelli, R. H. Page, and K. I. Schaffers, "0.5 W efficient broadly tunable continuous-wave Cr^{2+}:ZnSe laser," presented at the Adv. Solid State Lasers, Davos, Switzerland, 2000, Paper MC6.

[23] I. T. Sorokina, E. Sorokin, S. Mirov, V. Fedorov, V. Badikov, V. Panyutin, and K. I. Schaffers, "Broadly tunable compact continuous-wave Cr^{2+}:ZnS laser," *Opt. Lett.*, vol. 27, pp. 1040–1042, Jun. 15, 2002.

[24] I. T. Sorokina, E. Sorokin, S. Mirov, V. Fedorov, V. Badikov, V. Panyutin, A. Di Lieto, and M. Tonelli, "Continuous-wave tunable Cr^{2+}:ZnS laser," *Appl. Phys. B*, vol. 74, pp. 607–611, Apr. 2002.

[25] I. T. Sorokina, E. Sorokin, A. D. Lieto, M. Tonelli, R. H. Page, and K. I. Schaffers, "Active and passive mode-locking of Cr^{2+}:ZnSe laser," in *Proc. Adv. Solid-State Lasers*, 2001, pp. 157–161.

[26] I. T. Sorokina, E. Sorokin, and T. Carrig, "Femtosecond pulse generation from a SESAM mode-locked Cr:ZnSe laser," presented at the Conf. Lasers Electro-Opt./Quantum Electron. Laser Sci. Conf., Long Beach, CA, USA, 2006, Paper CMQ2.

[27] S. A. Payne and W. F. Krupke, "A glimpse into the laser-crystal ball," *Opt. Photon. News*, vol. 7, pp. 31–35, Aug. 1,1996.

[28] E. Sorokin, "Solid-state materials for few-cycle pulse generation and amplification," in *Few-Cycle Laser Pulse Generation and Its Applications*. vol. 95, F. X. Kärtner, Eds. Berlin, Germany: Springer, 2004, pp. 3–73.

[29] A. V. Podlipensky, V. G. Shcherbitsky, N. V. Kuleshov, V. I. Levchenko, V. N. Yakimovich, M. Mond, E. Heumann, G. Huber, H. Kretschmann, and S. Kück, "Efficient laser operation and continuous-wave diode pumping of Cr^{2+}:ZnSe single crystals," *Appl. Phys. B*, vol. 72, pp. 253–255, 2001.

[30] S. Kück, "Laser-related spectroscopy of ion-doped crystals for tunable solid-state lasers," *Appl. Phys. B*, vol. 72, pp. 515–562, 2001.

[31] I. T. Sorokina, E. Sorokin, A. D. Lieto, M. Tonelli, R. H. Page, and K. I. Schaffers, "0.5 W efficient broadly tunable continuous-wave Cr^{2+}:ZnSe laser," in Proc. Adv. Solid State Lasers, Davos, Switzerland, 2000, pp. 188–193.

[32] I. T. Sorokina, E. Sorokin, A. Di Lieto, M. Tonelli, R. H. Page, and K. I. Schaffers, "Efficient broadly tunable continuous-wave Cr^{2+}:ZnSe laser," *J. Opt. Soc. Am. B*, vol. 18, pp. 926–930, Jul. 2001.

[33] S. B. Mirov, V. V. Fedorov, I. Moskalev, S. Vasyliev, D. Martyshkin, M. Mirov, and V. P. Gapontsev, "Recent advances in high power, high energy tunable Cr:ZnS/Se lasers," presented at the Conf. Lasers Electro-Opt., San Jose, CA, USA, 2013, Paper CTu3D.1.

[34] S. B. Mirov, V. V. Fedorov, I. S. Moskalev, S. Vasilyev, D. V. Martyshkin, M. Mirov, and V. P. Gapontsev, "Recent progress in tunable Cr:ZnS/Se Lasers," presented at the Adv. Solid-State Lasers Congr., Paris, France, 2013, Paper JTh2A.64.

[35] E. Slobodchikov and P. F. Moulton, "1-GW-peak-power, Cr:ZnSe laser," presented at the Conf. Lasers Electro-Opt., Baltimore, MD, USA, 2011.

[36] E. Sorokin, N. Tolstik, and I. T. Sorokina, "1 Watt femtosecond mid-IR Cr:ZnS laser," *Proc. SPIE*, 2013, vol. 8599, p. 859916.

[37] I. T. Sorokina, V. V. Dvoyrin, N. Tolstik, and E. Sorokin, "Mid-IR ultrashort pulsed fiber-based lasers," *IEEE J. Sel. Topics Quantum Electron.*, vol. 20, no. 5, pp. 1–1, Sep./Oct. 2014.

[38] E. Sorokin, I. T. Sorokina, M. S. Mirov, V. V. Fedorov, I. S. Moskalev, and S. B. Mirov, "Ultrabroad continuous-wave tuning of ceramic Cr:ZnSe and Cr:ZnS lasers," in Proc. Adv. Solid-State Photon., San Diego, CA, USA, 2010, Paper AMC2.

[39] E. Sorokin, S. Naumov, and I. T. Sorokina, "Ultrabroadband infrared solid-state lasers," *IEEE J. Sel. Topics Quantum Electron.*, vol. 11, no. 3, pp. 690–712, May/Jun. 2005.

[40] I. T. Sorokina, "Cr^{2+}-doped II–VI materials for lasers and nonlinear optics," *Opt. Mater.*, vol. 26, pp. 395–412, 2004.

[41] A. Sennaroglu, U. Demirbas, H. Cankaya, N. Cizmeciyan, A. Kurt, and M. Somer, "Chromium-doped zinc selenide gain media: From synthesis to pulsed mid-infrared laser operation," *Proc. SPIE*, vol. 7598, pp. 75981B–1–75981B-10, 2010.

[42] T. J. Carrig, "Transition-metal-doped chalcogenide lasers," *J. Electron. Mater.*, vol. 31, pp. 759–769, 2002.

[43] A. Burger, K. Chattopadhyay, J. O. Ndap, X. Ma, S. H. Morgan, C. I. Rablau, C. H. Su, S. Feth, R. H. Page, K. I. Schaffers, and S. A. Payne, "Preparation conditions of chromium doped ZnSe and their infrared luminescence properties," *J. Crystal Growth*, vol. 225, pp. 249–256, 2001.

[44] V. I. Levchenko, V. N. Yakimovich, L. I. Postnova, V. I. Konstantinov, V. P. Mikhailov, and N. V. Kuleshov, "Preparation and properties of bulk ZnSe:Cr single crystals," *J. Crystal Growth*, vol. 198–199, pp. 980–983, 1999.

[45] J. O. Ndap, K. Chattopadhyay, O. O. Adetunji, D. E. Zelmon, and A. Burger, "Thermal diffusion of Cr^{2+} in bulk ZnSe," *J. Crystal Growth*, vol. 240, pp. 176–184, Apr. 2002.

[46] U. Demirbas, A. Sennaroglu, and M. Somer, "Synthesis and characterization of diffusion-doped Cr^{2+}:ZnSe and Fe2+:ZnSe," *Opt. Mater.*, vol. 28, pp. 231–240, Feb. 2006.

[47] I. T. Sorokina, "Crystalline mid-infrared lasers," in *Solid-State Mid-Infrared Laser Sources*. I. T. Sorokina and K. Vodopyanov, Eds. Berlin, Germany: Springer, 2003, vol. 89, pp. 262–358.

[48] V. I. Kozlovsky, Y. V. Korostelin, O. G. Okhotnikov, Y. P. Podmar'kov, Y. K. Skasyrsky, M. P. Frolov, and V. A. Akimov, "Intracavity laser spectroscopy with a semiconductor disk laser-pumped cw Cr^{2+}:ZnSe laser," *Quantum Electron.*, vol. 43, p. 885, 2013.

[49] N. Hempler, J. M. Hopkins, B. Rösener, M. Rattunde, J. Wagner, V. V. Fedorov, I. S. Moskalev, S. B. Mirov, and D. Burns, "Semiconductor disk laser pumped Cr^{2+}:ZnSe lasers," *Opt. Exp.*, vol. 17, pp. 18136–18141, 2009.

[50] J. T. Vallin, G. A. Slack, S. Roberts, and A. E. Hughes, "Infrared absorption in some II-VI compounds doped with Cr," *Phys. Rev. B*, vol. 2, pp. 4313–4333, 1970.

[51] J. T. Vallin, G. A. Slack, S. Roberts, and A. E. Hughes, "Near and far infrared absorption in Cr doped ZnSe," *Solid State Commun.*, vol. 7, pp. 1211–1214, 1969.

[52] A. Zunger, "Electronic structure of 3d transition-atom impurities in semiconductors," in *Solid State Physics*. E. Henry and T. David, Eds. New York, NY, USA: Academic Press, 1986, vol. 39, pp. 275–464.

[53] S. Kück, "Spectroscopy and laser characteristics of Cr^{2+}-doped chalcogenide crystals—Overview and recent results," *J. Alloys Compounds*, vol. 341, pp. 28–33, 2002.

[54] G. Huber, C. Kränkel, and K. Petermann, "Solid-state lasers: Status and future," *J. Opt. Soc. Am. B*, vol. 27, pp. B93–B105, Nov. 1, 2010.

[55] M. Kaminska, J. M. Baranowski, S. M. Uba, and J. T. Vallin, "Absorption and luminescence of Cr^{2+} (d^4) in II-VI compounds," *J. Phys. C, Solid State Phys.*, vol. 12, pp. 2197–2214, 1979.

[56] R. H. Page, J. A. Skidmore, K. I. Schaffers, R. J. Beach, S. A. Payne, and W. F. Krupke, "Demonstrations of diode-pumped and grating-tuned ZnSe:Cr2 +lasers," presented at the *Adv. Solid State Lasers*, Orlando, FL, USAY, 1997, Paper LS6.

[57] M. Mond, D. Albrecht, E. Heumann, G. Huber, S. Kück, V. I. Levchenko, V. N. Yakimovich, V. G. Shcherbitsky, V. E. Kisel, N. V. Kuleshov, M. Rattunde, J. Schmitz, R. Kiefer, and J. Wagner, "1.9-μm and 2.0-μm laser diode pumping of Cr^{2+}:ZnSe and Cr^{2+}:CdMnTe," *Opt. Lett.*, vol. 27, pp. 1034–1036, 2002.

[58] V. E. Kisel', V. G. Shcherbitsky, N. V. Kuleshov, V. I. Konstantinov, V. I. Levchenko, E. Sorokin, and I. Sorokina, "Spectral kinetic properties and lasing characteristics of diode-pumped Cr^{2+}: ZnSe single crystals," *Opt. Spectrosc.*, vol. 99, pp. 663–667, Oct. 2005.

[59] E. Sorokin and I. T. Sorokina, "Tunable diode-pumped continuous-wave Cr^{2+}:ZnSe laser," *Appl. Phys. Lett.*, vol. 80, pp. 3289–3291, May. 6, 2002.

[60] S. B. Mirov, V. V. Fedorov, K. Graham, I. S. Moskalev, I. T. Sorokina, and E. Sorokin, "Diode, fiber and potentially electrically pumped Cr^{2+}:ZnS mid-IR external cavity and microchip laser," presented at the 5th Int. Conf. Mid-Infrared Optoelectronics Mater. Devices, Baltimore, MD, USA, 2002.

[61] S. B. Mirov, V. V. Fedorov, K. Graham, I. S. Moskalev, I. T. Sorokina, E. Sorokin, V. Gapontsev, D. Gapontsev, V. V. Badikov, and V. Panyutin, "Diode and fibre pumped Cr^{2+}:ZnS mid-infrared external cavity and microchip lasers," *IEE P-Optoelectron.*, vol. 150, pp. 340–345, Aug. 2003.

[62] N. Kuleshov, M. Mond, E. Heumann, H. Kretschmann, S. Kueck, G. Huber, V. I. Levchenko, and V. N. Yakimovich, "Continuous wave diode pumped Cr^{2+}:ZnSe and high power laser operation," presented at the Adv. Solid-State Lasers, Seattle, WA, USA, 2001, Paper MC3.

[63] E. Slobodtchikov and P. Moulton, "Progress in ultrafast Cr:ZnSe lasers," presented at the Adv. Solid-State Photon., San Diego, CA, USA, 2012, Paper AW5A.4.

[64] J. B. McKay, W. B. Roh, and K. L. Schepler, "4.2 W Cr^{2+}:ZnSe face cooled disk laser," presented at the Conf. Lasers and Electro-Optics, Long Beach, CA, USA, 2002, Paper CMY3.

[65] K. L. Schepler, R. D. Peterson, P. A. Berry, and J. B. McKay, "Thermal effects in Cr^{2+}:ZnSe thin disk lasers," *IEEE J. Sel. Top. Quantum Electron.*, vol. 11, no. 3, pp. 713–720, May/Jun. 2005.

[66] G. Renz, J. Speiser, A. Giesen, I. T. Sorokina, and E. Sorokin, "Cr:ZnSe thin disk cw laser," *Proc. SPIE*, vol. 8599, p. 85991M, 2013.

[67] J. Speiser, G. Renz, and A. Giesen, "Thin disk laser in the 2 μm wavelength range," *Proc. SPIE*, vol. 8547, p. 85470E1, 2012.

[68] P. A. Berry, J. R. Macdonald, S. J. Beecher, S. A. McDaniel, K. L. Schepler, and A. K. Kar, "Fabrication and power scaling of a 1.7 W Cr:ZnSe waveguide laser," *Opt. Mater. Exp.*, vol. 3, pp. 1250–1258, Sep. 1, 2013.

[69] U. Demirbas and A. Sennaroglu, "Intracavity-pumped Cr^{2+}: ZnSe laser with ultrabroad tuning range between 1880 and 3100 nm," *Opt. Lett.*, vol. 31, pp. 2293–2295, 2006.

[70] A. Major, J. S. Aitchison, P. W. E. Smith, E. Sorokin, and I. T. Sorokina, "Z-scan characterization of the nonlinear refractive index of single crystal ZnSe in the 1.20–1.95 μm wavelength range," *Proc. SPIE*, vol. 5971, pp. 59710H–1–59710H-8, 2005.

[71] A. Major, F. Yoshino, J. S. Aitchison, P. W. E. Smith, E. Sorokin, and I. T. Sorokina, "Ultrafast nonresonant third-order optical nonlinearities in ZnSe for photonic switching at telecom wavelengths," *Appl. Phys. Lett.*, vol. 85, pp. 4606–4608, Nov. 15, 2004.

[72] M. Cizmeciyan, H. Cankaya, A. Kurt, and A. Sennaroglu, "Operation of femtosecond Kerr-lens mode-locked Cr:ZnSe lasers with different dispersion compensation methods," *Appl. Phys. B*, vol. 106, pp. 887–892, 2012.

[73] U. Morgner, W. Drexler, F. X. Kärtner, X. D. Li, C. Pitris, E. P. Ippen, and J. G. Fujimoto, "Spectroscopic optical coherence tomography," *Opt. Lett.*, vol. 25, pp. 111–113, 2000.

[74] B. Jean and T. Bende, "Mid-IR laser applications in medicine," in *Solid-State Mid-Infrared Laser Sources*. I. Sorokina and K. Vodopyanov, Eds. Berlin, Germany: Springer, 2003, vol. 89, pp. 530–565.

[75] W. S. Pelouch, G. J. Wagner, T. J. Carrig, and W. J. Scharpf, "Mid-wave ZGP OPOs pumped by a Cr:ZnSe laser," in *Proc. Adv. Solid-State Lasers*, 2001, p. PD1.

[76] K. Vodopyanov, E. Sorokin, P. Schunemann, and I. Sorokina, "4.4–5.4 μm frequency comb from a subharmonic OP-GaAs OPO pumped by a femtosecond Cr:ZnSe laser," presented at the Adv. Solid-State Photon., San Diego, CA, USA, 2011, Paper AME2.

[77] T. J. Carrig, G. J. Wagner, A. Sennaroglu, J. Y. Jeong, and C. R. Pollock, "Mode-locked Cr^{2+}:ZnSe laser," *Opt. Lett.*, vol. 25, pp. 168–170, 2000.

[78] I. T. Sorokina, E. Sorokin, A. D. Lieto, M. Tonelli, R. H. Page, and K. I. Schaffers, "Active and passive mode-locking of Cr^{2+}:ZnSe laser," presented at the Adv. Solid-State Lasers, Seattle, WA, USA, 2001, Paper MC2.

[79] E. Sorokin, I. T. Sorokina, A. D. Lieto, M. Tonelli, and P. Minguzzi, "Mode-locked ceramic Cr^{2+}:ZnSe laser," in *Proc. Adv. Solid-State Photon.*, 2003, pp. 227–230.

[80] D. J. Kuizenga and A. E. Siegman, "FM and AM mode locking of the homogeneous laser—Part I: Theory," *IEEE J. Quantum Electron.*, vol. QE-6, no. 11, pp. 694–708, Nov. 1970.

[81] J. Squier, F. Salin, S. Coe, P. Bado, and G. Mourou, "Characteristics of an actively mode-locked 2-psec Ti:sapphire laser operating in the 1-μm wavelength regime," *Opt. Lett.*, vol. 16, pp. 85–87, Jan. 1, 1991.

[82] D. E. Spence and W. Sibbett, "Femtosecond pulse generation by a dispersion-compensated, coupled-cavity, mode-locked Ti:sapphire laser," *J. Opt. Soc. Am. B*, vol. 8, pp. 2053–2060, Oct. 1, 1991.

[83] U. Keller, K. J. Weingarten, F. X. Kärtner, D. Kopf, B. Braun, I. D. Jung, R. Fluck, C. Hönninger, N. Matuschek, and J. Aus Der Au, "Semiconductor saturable absorber mirrors (SESAM's) for femtosecond to nanosecond pulse generation in solid-state lasers," *IEEE J. Sel. Topics Quantum Electron.*, vol. 2, no. 3, pp. 435–451, Sep. 1996.

[84] C. L. Cesar, M. N. Islam, C. E. Soccolich, R. D. Feldman, R. F. Austin, and K. R. German, "Femtosecond KCl:Li and RbCl:Li color-center lasers near 2.8 μm with a HgCdTe multiple-quantum-well saturable absorber," *Opt. Lett.*, vol. 15, pp. 1147–1149, 1990.

[85] C. Pollock, N. Brilliant, D. Gwin, T. J. Carrig, W. J. Alford, J. B. Heroux, W. I. Wang, I. Vurgaftman, and J. R. Meyer, "Mode locked and Q-switched Cr:ZnSe laser using a semiconductor saturable absorbing mirror (SESAM)," presented at the Adv. Solid-State Photon., Vienna, Austria, 2005, Paper TuA6.

[86] I. T. Sorokina, E. Sorokin, T. J. Carrig, and K. I. Schaffers, "A SESAM passively mode-locked Cr:ZnS laser," presented at the Adv. Solid-State Photon., Vancouver, Canada, 2006, Paper TuA4.

[87] I. T. Sorokina and E. Sorokin, "Chirped-mirror dispersion controlled femtosecond Cr:ZnSe laser," presented at the Adv. Solid-State Photon., Vancouver, Canada, 2007, Paper WA7.

[88] R. Szipöcs, C. Spielmann, F. Krausz, and K. Ferencz, "Chirped multilayer coatings for broadband dispersion control in femtosecond lasers," *Opt. Lett.*, vol. 19, pp. 201–203, Feb. 1, 1994.

[89] E. Sorokin and I. T. Sorokina, "Femtosecond operation and random quasi-phase-matched self-doubling of ceramic Cr:ZnSe laser," presented at the Conf. Lasers Electro-Opt., San Jose, CA, USA, 2010, Paper CTuGG2.

[90] E. Sorokin, N. Tolstik, and I. T. Sorokina, "Femtosecond operation and self-doubling of Cr:ZnS laser," presented at the Nonlinear Opt., Kauai, HI, USA, 2011, Paper NThC1.

[91] W. J. Tropf, "Temperature-dependent refractive index models for BaF_2, CaF_2, MgF_2, SrF_2, LiF, NaF, KCl, ZnS, and ZnSe," *Opt. Eng.*, vol. 34, pp. 1369–1373, 1995.

[92] V. L. Kalashnikov and E. Sorokin, "Soliton absorption spectroscopy," *Phys. Rev. A*, vol. 81, p. 033840, Jan. 2010.

[93] V. P. Gribkovskii, V. A. Zyulkov, A. E. Kazachenko, and V. A. Shakin, "Second harmonic generation on the grating of optical inhomogeneities in ZnSe and ZnS," *Phys. Status Solidi (B)*, vol. 159, pp. 379–385, 1990.

[94] M. Horowitz, A. Bekker, and B. Fischer, "Broadband second-harmonic generation in $Sr_xBa_{1-x}Nb_2O_6$ by spread spectrum phase matching with controllable domain gratings," *Appl. Phys. Lett.*, vol. 62, pp. 2619–2621, 1993.

[95] S. K. Kurtz and T. T. Perry, "A powder technique for the evaluation of nonlinear optical materials," *J. Appl. Phys.*, vol. 39, pp. 3798–3813, 1968.

[96] E. Y. Morozov, A. A. Kaminskii, A. S. Chirkin, and D. B. Yusupov, "Second optical harmonic generation in nonlinear crystals with a disordered domain structure," *JETP Lett.*, vol. 73, pp. 647–650, Jun. 1, 2001.

[97] M. Baudrier-Raybaut, R. Haïdar, P. Kupecek, P. Lemasson, and E. Rosencher, "Random quasi-phase-matching in bulk polycrystalline isotropic nonlinear materials," *Nature*, vol. 432, pp. 374–376, 2004.

[98] X. Vidal and J. Martorell, "Generation of light in media with a random distribution of nonlinear domains," *Phys. Rev. Lett.*, vol. 97, p. 013902, Jul. 7, 2006.

[99] S. Vasilyev, M. Mirov, and V. Gapontsev, "Kerr-lens mode-locked femtosecond polycrystalline Cr^{2+}:ZnS and Cr^{2+}:ZnSe lasers," *Opt. Exp.*, vol. 22, pp. 5118–5123, Mar. 10, 2014.

[100] E. Sorokin, N. Tolstik, K. I. Schaffers, and I. T. Sorokina, "Femtosecond SESAM-modelocked Cr:ZnS laser," *Opt. Exp.*, vol. 20, pp. 28947–28952, 2012.

[101] D. E. Spence, P. N. Kean, and W. Sibbett, "60-fsec pulse generation from a self-mode-locked Ti:sapphire laser," *Opt. Lett.*, vol. 16, pp. 42–44, Jan. 1, 1991.

[102] M. Piche and F. Salin, "Self-mode locking of solid-state lasers without apertures," *Opt. Lett.*, vol. 18, pp. 1041–1043, 1993.

[103] M. N. Cizmeciyan, H. Cankaya, A. Kurt, and A. Sennaroglu, "Kerr-lens mode-locked femtosecond Cr^{2+}:ZnSe laser at 2420 nm," *Opt. Lett.*, vol. 34, pp. 3056–3058, 2009.

[104] E. Sorokin and I. T. Sorokina, "Ultrashort-pulsed Kerr-lens modelocked Cr:ZnSe laser," presented at the Eur. Conf. Lasers Electro-Opt. Eur. Quantum Electron. Conf., München, Germany, 2009, Paper CF1_3.

[105] E. Sorokin, N. Tolstik, V. L. Kalashnikov, and I. T. Sorokina, "Chaotic chirped-pulse oscillators," *Opt. Exp.*, vol. 21, pp. 29567–29577, Dec. 2, 2013.

[106] N. Tolstik, E. Sorokin, and I. T. Sorokina, "Kerr-lens mode-locked Cr:ZnS laser," *Opt. Lett.*, vol. 38, pp. 299–301, 2013.

[107] N. Tolstik, I. T. Sorokina, and E. Sorokin, "Watt-level Kerr-lens mode-locked Cr:ZnS laser at 2.4 μm," presented at the Conf. Lasers Electro-Opt.: Sci. Innovations, San Jose, CA, USA, 2013, Paper CTh1H.2.

[108] B. Proctor, E. Westwig, and F. Wise, "Characterization of a Kerr-lens mode-locked Ti:sapphire laser with positive group-velocity dispersion," *Opt. Lett.*, vol. 18, pp. 1654–1656, 1993.

[109] E. Podivilov and V. L. Kalashnikov, "Heavily-chirped solitary pulses in the normal dispersion region: New solutions of the cubic-quintic complex Ginzburg-Landau equation," *JETP Lett.*, vol. 82, pp. 467–471, 2005.

[110] V. L. Kalashnikov, E. Podivilov, A. Chernykh, S. Naumov, A. Fernandez, R. Graf, and A. Apolonski, "Approaching the microjoule frontier with femtosecond laser oscillators: Theory and comparison with experiment," *New J. Phys.*, vol. 7, pp. 217–217, 2005.

[111] V. L. Kalashnikov, E. Podivilov, A. Chernykh, and A. Apolonski, "Chirped-pulse oscillators: Theory and experiment," *Appl. Phys. B*, vol. 83, pp. 503–510, 2006.

[112] V. L. Kalashnikov, E. Sorokin, and I. T. Sorokina, "Energy scaling of mid-infrared femtosecond oscillators," presented at the Adv. Solid-State Photon., Vancouver, Canada, 2007, Paper WE7.

[113] V. L. Kalashnikov, E. Sorokin, and I. T. Sorokina, "Energy-scalable mid-infrared femtosecond oscillators: Positive vs. negative dispersion regimes," presented at the Eur. Conf. Lasers Electro-Opt. Int. Quantum Electron. Conf., Munich, Germany, 2007, Paper CA2-4-MON.

[114] E. Sorokin, N. Tolstik, V. L. Kalashnikov, and I. Sorokina, "Chaotic regime in chirped-pulse mid-IR oscillators," presented at the Conf. Nonlinear Opt., Kohala Coast, HI, USA, 2013, Paper NF1A.7.

[115] V. L. Kalashnikov, E. Sorokin, and I. T. Sorokina, "Chaotic mode-locking of mid-IR chirped-pulse oscillator," presented at the Conf. Lasers Electro-Opt. Eur. 12th Eur. Quantum Electron. Conf., Munich, Germany, 2011, Paper CA.P.19 SUN.

[116] N. Tolstik, A. Pospischil, E. Sorokin, and I. T. Sorokina, "Graphene mode-locked Cr:ZnS chirped-pulse oscillator," *Opt. Exp.*, vol. 22, pp. 7284–7289, Mar. 24, 2014.

[117] N. Tolstik, I. T. Sorokina, and E. Sorokin, "Graphene mode-locked Cr:ZnS chirped-pulse oscillator," presented at the Adv. Solid-State Lasers Congr., Paris, France, 2013, Paper MW1C.2.

[118] E. Ugolotti, A. Schmidt, V. Petrov, J. Wan Kim, D. I. Yeom, F. Rotermund, S. Bae, B. Hee Hong, A. Agnesi, C. Fiebig, G. Erbert, X. Mateos, M. Aguiló, F. Diaz, and U. Griebner, "Graphene mode-locked femtosecond Yb:KLuW laser," *Appl. Phys. Lett.*, vol. 101, p. 161112, 2012.

[119] I. H. Baek, H. W. Lee, S. Bae, B. H. Hong, Y. H. Ahn, D.-I. Yeom, and F. Rotermund, "Efficient mode-locking of sub-70-fs Ti:sapphire laser by graphene saturable absorber," *Appl. Phys. Exp.*, vol. 5, p. 032701, 2012.

[120] Z. Sun, T. Hasan, and A. C. Ferrari, "Ultrafast lasers mode-locked by nanotubes and graphene," *Phys. E: Low-Dimensional Syst. Nanostructures*, vol. 44, pp. 1082–1091, Mar. 2012.

[121] M. N. Cizmeciyan, J. W. Kim, S. Bae, B. H. Hong, F. Rotermund, and A. Sennaroglu, "Graphene mode-locked femtosecond Cr:ZnSe laser at 2500 nm," *Opt. Lett.*, vol. 38, pp. 341–343, Feb. 1, 2013.
[122] M. N. Cizmeciyan, J. W. Kim, S. Bae, B. H. Hong, F. Rotermund, and A. Sennaroglu, "Graphene mode-locked Cr:ZnSe laser," presented at the Adv. Solid-State Lasers Congr., Paris, France, 2013, Paper MW1C.4.
[123] J. Ma, G. Xie, P. Lv, W. Gao, P. Yuan, L. Qian, U. Griebner, V. Petrov, H. Yu, H. Zhang, and J. Wang, "Wavelength-versatile graphene-gold film saturable absorber mirror for ultra-broadband mode-locking of bulk lasers," *Sci. Rep.*, vol. 4, p. 5016, 2014.
[124] N. Tolstik, E. Sorokin, and I. T. Sorokina, "Graphene mode-locked Cr:ZnS laser with 41 fs pulse duration," *Opt. Exp.*, vol. 22, pp. 5564–5571, Mar. 10, 2014.
[125] N. Tolstik, I. T. Sorokina, A. Pospischil, and E. Sorokin, "Graphene mode-locked Cr:ZnS laser with 44 fs pulse duration," presented at the Adv. Solid-State Lasers Congr., Paris, France, 2013, Paper MW1C.1.
[126] N. Tolstik, O. Okhotnikov, E. Sorokin, and I. T. Sorokina, "Femtosecond Cr:ZnS laser at 2.35 μm mode-locked by carbon nanotubes," *Proc. SPIE*, vol. 8959, pp. 89591A-89591A-6, 2014.
[127] N. Tolstik, E. Sorokin, and I. T. Sorokina, "Ceramic Cr:ZnS laser mode-locked by graphene," presented at the Conf. Lasers Electro-Opt., San Jose, CA, USA, 2014, Paper STu2E.7.
[128] A. Schliesser, N. Picque, and T. W. Hansch, "Mid-infrared frequency combs," *Nat. Photon.*, vol. 6, pp. 440–449, 2012.
[129] H. S. Margolis, "Spectroscopic applications of femtosecond optical frequency combs," *Chem. Soc. Rev.*, vol. 41, pp. 5174–5184, 2012.
[130] T. Udem, "Short and sharp - spectroscopy with frequency combs," *Science*, vol. 307, pp. 364–365, 2005.
[131] K. A. Tillman, R. R. J. Maier, D. T. Reid, and E. D. McNaghten, "Mid-infrared absorption spectroscopy across a 14.4°THz spectral range using a broadband femtosecond optical parametric oscillator," *Appl. Phys. Lett.*, vol. 85, p. 3366, 2004.
[132] A. Schliesser, M. Brehm, F. Keilmann, and D. van der Weide, "Frequency-comb infrared spectrometer for rapid, remote chemical sensing," *Opt. Exp.*, vol. 13, pp. 9029–9038, 2005.
[133] Z. Zhang, T. Gardiner, and D. T. Reid, "Mid-infrared dual-comb spectroscopy with an optical parametric oscillator," *Opt. Lett.*, vol. 38, pp. 3148–3150, Aug. 15, 2013.
[134] T. Ideguchi, B. Bernhardt, G. Guelachvili, T. W. Hänsch, and N. Picqué, "Raman-induced Kerr-effect dual-comb spectroscopy," *Opt. Lett.*, vol. 37, pp. 4498–4500, Nov. 1, 2012.
[135] V. L. Kalashnikov, E. Sorokin, and I. T. Sorokina, "Chirped dissipative soliton absorption spectroscopy," *Opt. Exp.*, vol. 19, pp. 17480–92, Aug. 29, 2011.
[136] J. Mandon, G. Guelachvili, I. T. Sorokina, E. Sorokin, V. L. Kalashnikov, and N. Picqué, "Enhancement of molecular dispersion spectral signatures in mode-locked lasers," presented at the 3rd EPS-QEOD Europhoton Conf., Paris, France, 2008, Paper WEoB.4.
[137] V. L. Kalashnikov, E. Sorokin, J. Mandon, G. Guelachvili, N. Picqué, and I. T. Sorokina, "Femtosecond Lasers for Intracavity Molecular Spectroscopy," presented at the 3rd EPS-QEOD Europhoton Conf., Paris, France, 2008, Paper TUoA.3.
[138] E. Sorokin, N. Tolstik, and I. T. Sorokina, "Enhancement and shape control of weak molecular absorption signal with chirped-pulse mid-IR lasers," presented at the Conf. Lasers Electro-Opt./Eur., Munich, Germany, 2013, Paper CD-1.2.
[139] N. Tolstik, E. Sorokin, V. Kalashnikov, and I. T. Sorokina, "Soliton delivery of mid-IR femtosecond pulses with ZBLAN fiber," *Opt. Mater. Exp.*, vol. 2, pp. 1580–1587, 2012.
[140] T. Skauli, K. L. Vodopyanov, T. J. Pinguet, A. Schober, O. Levi, L. A. Eyres, M. M. Fejer, J. S. Harris, B. Gerard, L. Becouarn, E. Lallier, and G. Arisholm, "Measurement of the nonlinear coefficient of orientation-patterned GaAs and demonstration of highly efficient second-harmonic generation," *Opt. Lett.*, vol. 27, pp. 628–630, 2002.
[141] K. L. Vodopyanov, O. Levi, P. S. Kuo, T. J. Pinguet, J. S. Harris, M. M. Fejer, B. Gerard, L. Becouarn, and E. Lallier, "Optical parametric oscillation in quasi-phase-matched GaAs," *Opt. Lett.*, vol. 29, pp. 1912–1914, 2004.
[142] K. L. Vodopyanov, E. Sorokin, I. T. Sorokina, and P. G. Schunemann, "Mid-IR frequency comb source spanning 4.4–5.4 μm based on subharmonic GaAs optical parametric oscillator," *Opt. Lett.*, vol. 36, pp. 2275–2277, Jun. 15, 2011.
[143] N. Leindecker, A. Marandi, R. L. Byer, and K. L. Vodopyanov, "Broadband degenerate OPO for mid-infrared frequency comb generation," *Opt. Exp.*, vol. 19, pp. 6296–6302, 2011.
[144] N. Leindecker, A. Marandi, R. L. Byer, K. L. Vodopyanov, J. Jiang, I. Hartl, M. Fermann, and P. G. Schunemann, "Octave-spanning ultrafast OPO with 2.6–6.1μm instantaneous bandwidth pumped by femtosecond Tm-fiber laser," *Opt. Exp.*, vol. 20, pp. 7046–7053, 2012.

Irina T. Sorokina was born in Moscow, Russia, in 1963. She received the Master's degree in physics and mathematics from the Lomonosov State University, Moscow, Russia, the Ph.D. degree in laser physics from the General Physics Institute of the Russian Academy of Sciences, Moscow, in 1992, and the Habilitation degree in quantum electronics and laser technology from the Technical University of Vienna, Vienna, Austria, in 2003.

Since 1991, she has been working as a Postdoctoral Researcher, and then as a University Lecturer and University Docent at the Technical University of Vienna. Since 2007, she has been a Full Professor of physics at the Norwegian University of Science and Technology, Trondheim, Norway, where she is currently leading a Laser Physics group, concentrating on the development of femtosecond solid-state and fiber lasers based on novel materials. She has authored and co-authored more than 300 publications, among which more than 100 peer-reviewed journal publications and book-chapters, and co-edited several books.

Dr. Sorokina was awarded the Snell Premium IEE Award for her contributions to the development of Cr:ZnS/Cr:ZnSe lasers in 2005. She is the Fellow of the Optical Society of America since 2006, and an elected Member of the Norwegian Academy of Science and Letters since 2009.

Evgeni Sorokin was born in 1962 in Moscow, Russia. He received the Master's degree in physics and mathematics from M. V. Lomonosov State University, Moscow, Russia, in 1986, the Ph.D. degree in laser physics and the Habilitation degree in quantum electronics and laser technology from Vienna University of Technology, Vienna, Austria, in 1994 and 2005, respectively.

Currently, he is a Professor of electrical engineering at the Photonics Institute, Vienna University of Technology. His current research interests include novel ultrabroadband laser materials, nonlinear optics, development of femtosecond solid-state lasers, and laser spectroscopy applications. He has authored and co-authored more than 300 publications, among which more than 100 peer-reviewed journal publications and book chapters, and co-edited several books.

Dr. Sorokin was awarded the Snell Premium IEE Award for contributions to the development of Cr:ZnS/Cr:ZnSe lasers in 2005. He is a Member of the OSA and the EPS.